THE UNIVERSITY OF
SYDNEY

COPYRIGHT AND USE OF THIS THESIS

Soft Information Based Protocols
in Network Coded Relay Networks

Yiwen Li

A thesis submitted in fulfilment of
the requirements for the degree of Master of Philosophy
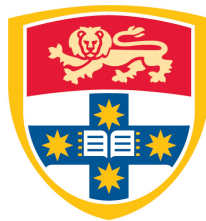
Engineering & IT
The University of Sydney

Jul 2014

Abstract

Future wireless networks aim at providing higher quality of service (QoS) to mobile users. However, phenomena such as multipath fading and limited resources, namely bandwidth, still constrain almost every design. The emergence of relay technologies has shed light on new methodologies through which the system capacity can be dramatically increased with low deployment cost. In this thesis, novel relay technologies have been proposed in two practical scenarios: wireless sensor networks (WSN) and cellular networks. The research includes theoretical analysis and simulations performed to show the advantages of the proposed protocols over existing relay protocols.

In practical WSN designs, energy conservation is the single most important requirement; being powered by batteries and deployed in distributed areas, designs aim at extending the life span of the sensor network by reducing its energy consumption. Often, replacing or recharging batteries is too difficult or even impossible; thus extending the life span of the network would reduce maintenance costs. The introduction of relay nodes to the WSN has much relieved the burden of each source node. This is because the relay nodes are usually more powerful and being deployed in the middle of the remote transmissions, which can assist to forward messages from the source nodes. At the same time, because adjacent source nodes are observing the same phenomenon, there should be a lot of redundancy within the data they have gathered. Relay nodes can thus eliminate the redundancy through processing the received signals together. This thesis draws attention to a multiple access relay channels (MARC) model in the WSN, where two correlated source nodes transmit their messages to a common destination via the help of a relay node. Network coding (NC) is performed at the relay node by merging two received signals into one signal using predetermined techniques. In this thesis, the network coded symbol for the received signals from correlated sources has been derived; the network coded symbol vector is then converted into a sparse vector, after

which a compressive sensing (CS) technique is applied over the sparse signals. A theoretical proof analysis is derived regarding the reliability of the network coded symbol formed in the proposed protocol. This reliability is compared to the one for the conventional estimate-and-forward (EF) protocol. The proposed protocol results in a better bit error rate (BER) performance in comparison to the direct implementation of CS on the EF protocol. Simulation results validate our analyses. Additionally, as less number of signals are transmitted from the relay node due to CS, the overall transmission time is reduced and thus the system throughput is improved.

Another hot topic is the application of relay technologies to the cellular networks. In this thesis, a two-way relay channels (TWRC) model is considered, where two source mobile users exchange their information via the help of a third mobile user. In the existing relay protocols, the soft information forwarding (SIF) protocols stand out, as they can achieve a better error performance by forwarding the intermediate soft decisions at the relay. The soft information can be in the form of estimates of the source signals or the mutual information of the received signals. However, in practical scenarios, the delivery of soft information takes a lot of bandwidth. Even if we quantize the soft information into a few bits, the loss of precision and the expanded bandwidth requirement decrease the quality of service of these SIF protocols. In this thesis, a practical two-way transmission scheme is proposed based on the EF protocol and the network coding technique. A trellis coded quantization/modulation (TCQ/M) scheme is used in the network coding process, because the TCQ uses a structured codebook with an expanded set of quantization levels then the quantization noise can be reduced without rate increasing. The soft network coded symbols are quantized into only one bit thus requiring the same transmission bandwidth as the simplest decode-and-forward (DF) protocol. The probability density function (PDF) of the network coded symbol is derived to help to form the quantization codebook for the TCQ. Moreover, an adaptive codebook is proposed for the TCQ/M scheme under different channel conditions. Simulations show that the proposed soft forwarding protocol can achieve full diversity with only a transmission rate of 1, and its BER performance is equivalent to that of an unquantized EF protocol.

Acknowledgements

Statement of Originality

All materials presented in this thesis are the original work of the author, while enrolled in the School of Electrical and Information Engineering at the University of Sydney as a candidate for the Master of Philosophy. The content of this thesis has not been previously submitted for examination as part of any academic qualifications. Most of the results contained herein have been published, accepted for publication, or submitted for publication, in journals or conferences of international standing. The author's contribution in terms of the published material is listed in next section "Related Publications".

This work was conducted under the joint supervision of Professor Branka Vucetic and Dr. Zihuai Lin at the School of Electrical and Information Engineering, the University of Sydney, Australia.

Yiwen Li
School of Electrical and Information Engineering
The University of Sydney, Australia
Jul 2014

Related Publications

Journal Papers

[J1] Y. Li, J. Li, Z. Lin, Y. Li, and B. Vucetic, "Compressive Soft Forwarding in Network Coded Multiple Access Relay Channels," *IEEE Trans. Veh. Technol.*, submitted for publication.

Conference Papers

[C1] Y. Li, Z. Lin, J. Li and B. Vucetic, "A Soft Information Delivery Scheme in Two-Way Relay Channels with Network Coding," in *Proc. IEEE PIMRC*, London, Sep. 2013, pp. 100-104.

[C2] Y. Li, J. Li, Z. Lin, Y. Li and B. Vucetic, "Network Coded Soft Forwarding for Multiple Access Relay Channels with Compressive Sensing," *IEEE ICC 2014*, accepted for publication.

Contents

List of Figures

List of Acronyms

AF	Amplify-and-Forward
APP	A Posterior Probability
AWGN	Additive White Gaussian Noise
BCJR	Bahl-Cocke-Jelinek-Raviv
BER	Bit Error Rate
BP	Belief Propagation
BPSK	Binary Phase-Shift Keying
CEF-CS	Correlated Estimate-and-Forward with Compressive Sensing
CS	Compressive Sensing
CSI	Channel State Information
DF	Detect-and-Forward
EF	Estimate-and-Forward
FFT	Fast Fourier Transform
i.i.d.	independent and identically distributed
LLR	Log-likelihood Ratio
MAP	Maximum a Posteriori
MARC	Multiple Access Relay Channels
MMSE	Minimum Mean Square Errors
NC	Network Coding
PDF	Probability Density Function
PNC	Physical Layer Network Coding
QoS	Quality of Service
QPSK	Quadrature phase-shift keying
SIF	Soft Information Forwarding
SMI	Symbol-Wise Mutual Information
SNR	Signal-to-Noise Ratio

SQNR	Signal-to-Quantization-Noise Ratio
TCM	Trellis Coded Modulation
TCQ	Trellis Coded Quantization
TWRN	Two-Way Relay Network
VA	Viterbi Algorithm
WSN	Wireless Sensor Networks

List of Notations

d	Euclidean distance
E_i	transmission power at $\mathcal{S}_i$
$E_{\mathcal{R}}$	relay transmission power
$E_{\mathcal{S}}$	source transmission power
$f_{\mathrm{AF}}()$	relay function of the AF protocol
$f_c()$	convolution operation
$f_{\mathrm{DF}}()$	relay function of the DF protocol
$f_{\mathrm{EF}}()$	relay function of the EF protocol
h	fading channel coefficient
k	sparsity
l	signal length
m	number of measurements in compressive sensing
$\boldsymbol{n}$	noise sample vector
$n_c \backslash v$	the set of variables in n_c with n_v excluded
p	probability density function
$q_{v \to c}$	messages sent from the variable nodes to constraint nodes in BP
$Q()$	Q function
R	rate in trellis coding
r	transmission rate in compressive sensing
$r_{c \to v}$	messages sent from the constraint nodes to variable nodes in BP
s	channel signal
$\tanh$	hyperbolic tangent: $\tanh x = \frac{1 - e^{-2x}}{1 + e^{-2x}}$
Tr	throughput
$V(c)$	the set of variable nodes that the cth constraint node n_c depends on
$V(c) \backslash v$	the set $V(c)$ with variable node n_v excluded
$\boldsymbol{x}$	transmitted signal vector

$\boldsymbol{x}^*$	non-increasing arrangement of the vector $\boldsymbol{x}$
$\boldsymbol{x}_{\mathcal{R}}$	network coded symbol vector
$\hat{x}_i^q$	hard decision on the q-th symbol of the transmitted symbol vector at $\mathcal{S}_i$
$\hat{x}_{\mathcal{R}}^q$	hard decision on the q-th symbol in the network coded symbol vector
x_i^q	the q-th symbol in the signal vector transmitted from $\mathcal{S}_i$
$\boldsymbol{y}$	received signal vector
$\mathcal{E}$	expectation operation
σ^2	variance of the noise sample
ζ	correlation coefficient
τ	correlation related parameter
$\mathcal{C}$	codebook
$\mathcal{B}$	power normalization
$\mathcal{S}$	state space in trellis
$\boldsymbol{\Psi}$	orthonormal basis for a sparse signal
$\boldsymbol{\theta}$	nonzero entries vector of a sparse signal
$\boldsymbol{\Phi}$	encoding matrix in compressive sensing
$\boldsymbol{\Phi}^*$	conjugate of $\boldsymbol{\Phi}$
$\lVert\cdot\rVert_p$	l_p norm
$\emptyset$	empty set
$\mathcal{O}$	large O: $f(x) = \mathcal{O}(g(x))$, if and only if there exists a positive real M and a real number x_0 such that $\lvert f(x)\rvert < M\lvert g(x)\rvert$, for all $x > x_0$ $\lim\limits_{x\to x_0}\dfrac{f(x)}{g(x)} = 0$

Chapter 1

Introduction

This Chapter presents the background information and motivation for our research topics, and briefly formulates the research problems underlying the industrial needs. Further, major contributions of this thesis are listed, and followed by a concise outline of the thesis.

1.1 Wireless Relay Networks

In wireless networks, signal fading resulting from multipath propagation becomes a severe channel impairment. To mitigate the influence of signal fading, the use of diversity is thus proposed. There are a variety of diversity forms, including spatial diversity, temporal diversity, and frequency diversity [1]. Space diversity is most attractive because it does not use the precious communication resources, as time and frequency diversity do; besides, even when such other forms of diversity are not available, space diversity can still provide superb performance gains. The underlying principle of spatial diversity is that geographically separated transmitters transmit signals to geographically separated receivers, and these signals will experience independent fading conditions through separate channels. Works in [2–4] indicate that multiple antennas can offer the spacial diversity; however, in future cellular networks or wireless sensor networks, due to the size and hardware implementation constraints, a compact mobile terminal or wireless sensor node may not be capable of supporting multiple antennas [5]. Authors in [6] proposed a new form of spatial diversity whose purpose is

Figure 1.1: A future cooperated cellular network.

to combat this constraint while still emulate the antenna diversity. They proposed that, the wireless users in cellular or ad hoc variety cooperate with each other, aiming to achieve the diversity gains. Therefore, users can be regarded as the relay nodes, and each of the cooperated users takes responsibility for not only the transmission of its own messages, but also the messages of other users.

The cooperative communication can be tracked back to the first relay model introduced in 1971 in [7]. Back then it was a special form of a three-terminal network. Then the groundbreaking work on information theoretic properties of the relay channels was given by authors in [8] where the system model was also a simple three-terminal network consisting of a source, a destination and a relay. However, on one hand, for wireless communication systems, the analysis made in [7, 8] only considered additive white Gaussian noise (AWGN) channel, and this does not apply to the fading channels. On the other hand, the users are playing a more important role in cooperative communication, as they are working as both the information sources and the relays, which differs from the totally independent role of the relay node back in 1970s. The state-of-the-art relay-based technologies are vital to many applications. In the cellular systems, as the data throughput in mobile communication networks

is increasing dramatically, as well as the number of mobile users located in cells, it is high time that we took advantage of the limited frequency spectrum and the scarce bandwidth resource [9–11]. Moreover, standardization organizations already included relay-based cooperative networks in the 3rd Generation Partnership Project (3GPP) [12]. Fig. 1.1 depicts one possible future cellular network where relay nodes are deployed near the edge of the cell to solve the coverage problem for high data rates. With regard to ad-hoc networks, one attractive branch is the wireless sensor networks (WSN) [13]. Researchers also proposed to deploy a small number of relay nodes in the large scale WSN, in order to prolong the network life span, thus achieving energy conservation [14, 15].

1.2 Research Problems

Given the nature and features of wireless communication channels and the anticipated demand for future wireless networks with high data transmission rate, it is crucial to design bandwidth-efficient techniques which can help to mitigate any limiting effects of the wireless channels. In this thesis, one soft information relaying protocol for correlated sources is proposed, and one practical soft information delivery scheme is proposed.

1.2.1 Network Coding for Physical Layer Communications

The notion of network coding (NC) was first introduced as a network layer multicasting technique in computer networks [16]; the nodes do not directly forward packets received, instead, they combine packets together before further transmission. Compared with conventional transmission methodology, network coding has been proved to improve networks' efficiency, throughput and robustness [17, 18]. Recently, to further enhance the capacity of physical layer relaying channels, network coding has been applied to cooperative relay networks [19, 20], and protocols aiming for these networks are generally referred to as physical layer network coding (PNC) protocols [21, 22]. The underlying principle of PNC is that the relay nodes in the network combine multiple messages received from physical-layer transmission [23]. Compared with NC in computer networks where intermediate nodes combine digital signals, the PNC protocols take advantage of the analog signals from various source

nodes for combination [22].

Two classical relay protocols, namely, amplify-and-forward (AF) [24] and decode-and-forward (DF) [25], have been widely investigated in PNC. However, in the AF protocol, the relay amplifies the incoming signal and forwards it to the destination, resulting in the noise amplification at the relay; in the DF protocol, the relay decodes the received signal, re-encodes it and then forwards it to the destination. Its drawback is that it propagates the erroneous decisions to the destination. Consequently, a new relaying concept, namely, soft information forwarding (SIF) has been proposed to achieve a better error performance by forwarding the intermediate soft decisions at the relay [26–29]. The soft information can be in the form of log-likelihood ratio (LLR) [26], soft symbol [27], or soft mutual information [28, 29].

However, these SIF protocols are investigated in one-way or two-way relay channels, which are not directly applicable for general multi-source relay channels, where multiple sources communicate with their destination with the help of the relay. Multiple access relay channels (MARC) are common and basic building blocks in wireless networks, such as WSN [13]. In the MARC, wireless network coding has been applied to enhance the network performance [30, 31]. Besides, in WSN, it is common that two sources in the MARC transmit correlated information. This is because neighboring sensor nodes obtain spatially correlated measurements, and the problem of the sensor reachback problem on how to efficiently transmit correlated data from multiple source nodes to one or multiple destination nodes, has been investigated recently [32, 33]. When NC is applied at the relay, the network coded symbols of the correlated sources contain redundant information, which can be compressed before being forwarded to the destination. However, the current SIF protocols only consider uncorrelated sources. Then how to efficiently reduce the redundancy in the network coded signals at the relay nodes becomes a worthy research problem.

1.2.2 Delivery of Soft information

In terms of the soft-symbol based SIF protocol in [27], also known as estimate-and-forward (EF), the relay node forms the soft symbols by calculating the minimum mean squared errors (MMSE) estimates of the received symbols at the relay. The MMSE estimates of the received symbols are referred to as the expectation of the transmitted symbols on condition of the received signals at the relay. It is shown in [27] that the EF protocol maximizes the signal-

to-noise ratio (SNR) at the destination and thus gains a better error performance compared to the AF and DF protocols. Another recent soft information relaying protocol is referred to as mutual information forwarding (MIF) [28, 29, 34, 35], where the relay nodes forward symbol-wise mutual information (SMI) to the destination. Results in [34] have shown that the MIF protocol can achieve better error performance compared to the EF protocol.

The research of relay protocols has been extended to more complicated wireless networks, such as the two-way relay channels (TWRC) whose model will be discussed in the following chapter. This model has recently attracted much attention due to its promising application to future wireless cooperation systems [28, 36–39], such as, two mobile users exchanging their own information via a third mobile user. Hence relay protocols targeting at TWRC have emerged, including an EF based soft network coding protocol proposed in [38], and two MIF based protocols, namely, network-coded MIF and superposition-coded MIF proposed in [28].

These SIF protocols are all proved to outperform both AF and DF protocols over fading TWRC. However, an assumption is made within the SIF protocols, that soft information at the relay nodes can be directly forwarded to the destination through the bandwidth limited channels. This is impractical for real systems because continuous real numbers require an increased bandwidth, which is unacceptable in a bandwidth limited network. Apart from this, even if we are capable of quantizing such soft information into a few bits, compared with the traditional DF protocol which only requires a transmission rate of 1, and the AF protocol which can be easily implemented without any computing, the SIF protocols still appear to be flawed.

1.3 Contributions of the thesis

In this thesis, novel designs for relay protocols have been proposed, and further validated by rigorous mathematical analysis and extensive simulations. In relation to the two major research problems, contributions are classified into the following two parts.

With regard to increasing transmission efficiency of correlated sources, I have made the following contributions.

1. The soft symbol expression at the relay node, with the sources' correlation informa-
   tion, is derived. When the EF protocol is designed for multiple sources, source signals
   are regarded as independent. However, in WSN where adjacent sensor nodes collect
   correlated information, it is extremely energy-consuming to adopt conventional relay
   protocols where independent sources are considered. Based on the principle of the EF
   protocol, we still calculate the MMSE estimates of the received signal but consider the
   source correlation information. We analytically show that, the soft symbols obtained
   from the proposed protocol have higher reliability than those calculated in the EF pro-
   tocol, except for the scenario where sources are independent to each other. In the latter
   case, the soft symbols in these two SIF protocols are exactly the same.

2. When the source nodes are correlated, based on the simulation and observation of the
   probability density function (PDF) of the soft symbol obtained at the relay node, we
   find out that the soft symbol vector can be easily converted into a sparse vector by sub-
   tracting one from each soft symbol. The definition of sparsity drives us to implement
   compressive sensing (CS), which is an efficient and attractive tool at the cutting edge
   of signal processing. Belief propagation (BP) is performed at the decoding side, being
   able to decode both strictly sparse signal and approximately sparse signal transmitted
   from the relay node. We define our proposed signal as correlated estimate-and-forward
   with compressive sensing (CEF-CS) protocol. To our best knowledge, this is by far
   the first work to concatenate CS with the relay networks.

3. Simulations show that the source correlation has a great impact on the performance
   of the proposed protocol. Specifically, as long as the source correlation is below a
   certain level, the proposed protocol can achieve full diversity. In addition, when the
   source correlation is fixed to a value corresponding to the full diversity, simulations
   demonstrate that the compression rate is directly linked to the BER performance of
   the CEF-CS protocol. In particular, the higher the compression rate is, the worse the
   performance will be. There also exists a certain threshold, beyond which the system
   can no longer achieve full diversity. It is important to note that with highly correlated
   source model and a compression rate of 0.3, the CEF-CS protocol can achieve the
   same BER as the conventional EF protocol, while it consumes much less transmission
   time due to the compression at the relay node; thus the throughput performance of the
   system is much improved.

For the practical delivery scheme of the SIF protocols, our contributions are as follows.

1. We take advantage of the trellis coded quantization/modulation (TCQ/M) to quantize the soft bits obtained from the EF protocol into 1 bit. To our best knowledge, this is the first attempt to adopt a source coding method at a relay node aiming at the compression.

2. The probability density function expression of the networked coded soft symbol in the EF protocol is derived for the TWRC. The PDF expression is further exploited by the Lloyd-Max quantizer, and being used to determine the quantization levels of the TCQ.

3. We propose to use adaptive codebooks for the TCQ/M system according to different channel conditions. Specifically, when the source-to-relay channel SNR is in relatively low region, the codebooks for the TCQ/M are generated by a Lloyd-Max quantizer based on the PDF of the soft symbols; when the source-to-relay channel SNR is high, the codewords are repeated in a codebook in order to ensure that erroneous mapping is avoided in the trellis of the TCQ.

4. Simulations verify that, with transmission rate 1, the DF protocol has only the diversity gain of 1, but the proposed 1-bit soft forwarding protocol can achieve the full diversity. Furthermore, the proposed protocol has about 1 dB coding gain compared to the AF protocol at a BER of 10^{-3}.

1.4   Thesis Outline

This thesis is composed of five Chapters, including the background information, research designs, corresponding simulation results, and conclusions we draw from the research. The structure is briefly summarized as follows:

Chapter 1 contains background knowledge, research problems and major contributions of this thesis.

Chapter 2 presents the preliminary knowledge, including existing relay protocols, trellis codes and compressive sensing, laying a foundation for the subsequent Chapters.

Chapter 3 proposes a novel estimate-and-forward protocol in MARC where two correlated sources transmit their information to the common destination with the help of a relay. We convert the network coded soft symbol vector at the relay nodes into a sparse vector and adopt CS over the sparse signal. We also analyze the performance of the proposed CEF-CS protocol by comparing the soft symbol value and received signal-to-noise ratio with the conventional EF protocol. Simulations show that our protocol can achieve the same BER as the conventional EF protocol with proper compression rates, while it consumes much less transmission time due to the compression.

Chapter 4 proposes a practical 1-bit soft forwarding protocol for a network-coded two-way relay channel, which solves the soft information delivery problem for the EF protocol. We concatenate the TCQ/M scheme with the relay network, and design an adaptive codebook for the TCQ scheme in order to achieve good error performance. Simulations show that our 1-bit soft forwarding protocol outperforms both the DF and the AF protocols, and well approximates the conventional EF protocol without any quantization.

Chapter 5 concludes the thesis by summarizing the major contributions and findings.

Chapter 2

Background

The first part of this chapter provides a brief review of the popular relay network types and major relay technologies that are crucial to the understanding of Chapter 3 and 4. Relay functions in terms of different strategies are given, providing benchmarks as well as solid foundations for the proposed relay protocols in Chapter 3 and 4.

The second part of this chapter discusses a signal processing tool called compressive sensing. Several reconstruction algorithms of CS have been involved and compared, among which a belief propagation decoding algorithm under the Bayesian framework draws our attention, leading to the essential part of our decoder design in Chapter 3.

The third part talks about a joint source/channel coding technique, referred to as trellis coded quantization/modulation. Channel coding and source coding have been reviewed respectively, followed by a joint system. The Viterbi algorithm is also reviewed for better understanding of the notion of trellis coding.

2.1 Relay Cooperation

2.1.1 Relay Models

According to various applications, the introduction of relay nodes has enabled the study of different relay models and different deployments of the relay nodes. In this section, we will introduce two popular and practical relay models, namely two-way relay channels and multiple access relay channels.

2.1.1.1 Two-way Relay Channels

TWRC have attracted a lot of attention from both academia and industries [40, 41]. The concept of a TWRC model is that two source nodes communicate with each other with the help of another relay node or other relay nodes. This model can be easily extended to mobile communication within cellular networks where two mobile users exchange their information with the aid of a third mobile user. Initially, the exchange of bidirectional information was completed in a transmission period of four time slots [42]. Specifically, one source sends its own message to the other source and the relay in the first time slot, and the relay helps to forward the received signal to the other source in the second time slot, then during the third and fourth time slots the other source transmits its message in the same way. However, such a system leads to a problem that the introduction of relay nodes degrades the overall throughput performance [23, 43].

In order to improve the spectral efficiency, works in [16–18] raised that the two source nodes can complete communication within three time slots, with the help of network coding. NC is introduced in [44] aiming to exploit the characteristics of the wireless medium, in particular, the broadcast nature of the wireless channel, in order to increase the throughput of the entire network. A typical TWRC model with three-time-slot transmission is shown in Fig. 2.1. Within the first two time slots, either source transmits their own messages to the relay and the other source, respectively. During the third time slot, the relay forms the network coded symbols and transmits these signals back to both sources [45].

The throughput performance can be further enhanced by enabling two sources to transmit
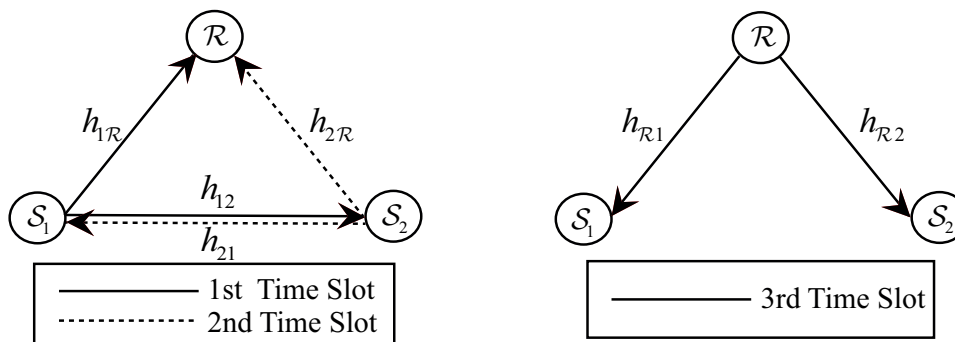
Figure 2.1: A two-way relay network.

their signals simultaneously to the relay and their counterpart. Therefore, this can be accomplished within one time slot [21]; within the next time slot, the relay transmits the formed network coded symbols back to both sources. With less time slots being used for transmission, such a two-time-slot scheme can achieve higher spectral efficiency than the three-time-slot scheme [41, 46].

2.1.1.2   Multiple Access Relay Channels

In conjunction with network coding, another PNC scheme is referred to as multiple access relay channels. The simplest MARC is shown in Figure 2.2, which consists of only two source nodes, one relay node and one destination node.

A general MARC system can be used for the cooperative uplink for multiple mobile stations to a base station with the help of a relay [47], or can be extended to WSN where multiple sensors transmit message to the remote server via the help of the more powerful relay node. Another example to explain the simplest MARC is that two mobile users communicate with a base station using a third mobile user as a relay node in a cellular system. As described in [48], the relay node can even be a fixed node settled in higher locations such as street light posts and roof tops in metropolitan mesh network applications,.

In a general MARC, multiple sources transmit their messages to a common destination with the help of a single relay. As MARC is based on the realization of network coding, the relay node merges the messages received from the sources and forwards them to the destination. A general MARC model can be found in [49]. And the capacity bound for the general MARC, where the sources and the relay can transmit simultaneously is given in [50].
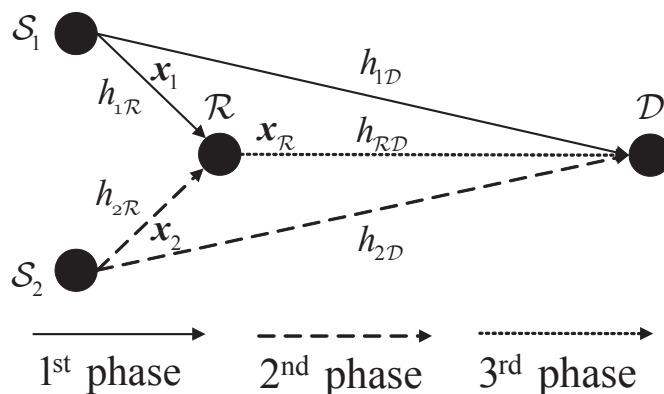
Figure 2.2: The orthogonal uplink relay channel with two sources, one relay, and one destination.

2.1.2 Relay Protocols

We review the relay functions of the amplify-and-forward, the decode-and-forward and the estimate-and-forward protocols in this section. We consider about the two sources and one relay scenario, namely $\mathcal{S}_1$, $\mathcal{S}_2$ and $\mathcal{R}$, in the source-to-relay channels in either the TWRC shown in Fig. 2.1 or the MARC shown in Fig. 2.2.

We denote by $h_{i\mathcal{R}}$, $i = 1, 2$, the channel coefficients between $\mathcal{S}_i$ and $\mathcal{R}$. We assume that each source transmits l independent and identically distributed (*i.i.d.*) binary phase-shift keying (BPSK) symbols. Thus, the symbol vector of $\mathcal{S}_i$ is denoted by $\boldsymbol{x}_i = (x_i^1, \cdots, x_i^l)^T$, $x_i^q \in \{\pm 1\}$ and $q \in \{1, \cdots, l\}$, with the power E_i. The received signals at the relay from $\mathcal{S}_i$ can be expressed as

$$\boldsymbol{y}_{i\mathcal{R}} = h_{i\mathcal{R}} \sqrt{E_i} \boldsymbol{x}_i + \boldsymbol{n}_{i\mathcal{R}}, \tag{2.1}$$

where the vector $\boldsymbol{y}_{i\mathcal{R}}$ consists of l received signals, i.e., $\boldsymbol{y}_{i\mathcal{R}} = (y_{i\mathcal{R}}^1, \cdots, y_{i\mathcal{R}}^l)^T$, and the vector $\boldsymbol{n}_{i\mathcal{R}} = (n_{i\mathcal{R}}^1, \cdots, n_{i\mathcal{R}}^l)^T$ consists of l additive white Gaussian noise (AWGN) samples at the relay. We assume the noise sample at the relay is independent and identically distributed (*i.i.d.*) with a mean zero and variance σ^2, and the sources' power satisfies $E_1 = E_2 = E_\mathcal{S}$.

When the AF protocol is applied, the task of the relay node is to superimpose the received signals from the two sources, and then broadcast the superposition in the next stage of the transmission. Therefore in the AF protocol, the relay function for each network coded sym-

bol can be expressed as

$$f_{\mathrm{AF}}(y_{1\mathcal{R}}^q, y_{2\mathcal{R}}^q) = \sqrt{\frac{1}{2\left(E_{\mathcal{S}} + \sigma^2\right)}}(y_{1\mathcal{R}}^q, y_{2\mathcal{R}}^q). \tag{2.2}$$

For the DF protocol, the relay makes hard decisions on the symbols x_1^q and x_2^q, and then obtains the network coded symbol according to the hard decisions $\hat{x}_1^q$ and $\hat{x}_2^q$. We define the network coded symbol vector as $\boldsymbol{x}_{\mathcal{R}} = (x_{\mathcal{R}}^1, \cdots, x_{\mathcal{R}}^l)^T$, $x_{\mathcal{R}}^q \in \{\pm 1\}$; then a network coded symbol $x_{\mathcal{R}}^q$ in $\boldsymbol{x}$ is defined as $x_{\mathcal{R}}^q \triangleq x_1^q x_2^q$. So the hard decision of $x_{\mathcal{R}}^q$ can be calculated as $\hat{x}_{\mathcal{R}}^q = \hat{x}_1^q \hat{x}_2^q$. Thus for the DF protocol, the relay function can be given by

$$f_{\mathrm{DF}}(y_{1\mathcal{R}}^q, y_{2\mathcal{R}}^q) = \hat{x}_{\mathcal{R}}^q = \hat{x}_1^q \hat{x}_2^q. \tag{2.3}$$

In terms of the EF protocol, the minimum mean squared error (MMSE) estimation of $x_{\mathcal{R}}^q$ is calculated at the relay nodes, namely the conditional expectation of $x_1^q x_2^q$ based on $y_{1\mathcal{R}}^q$ and $y_{2\mathcal{R}}^q$: $\mathcal{E}\left(x_1^q x_2^q | y_{1\mathcal{R}}^q, y_{2\mathcal{R}}^q\right)$. Due to the independence of the received $y_{1\mathcal{R}}^q$ and $y_{2\mathcal{R}}^q$, the MMSE estimation at the relay is given by [38]

$$\mathcal{E}\left(x_1^q x_2^q | y_{1\mathcal{R}}^q, y_{2\mathcal{R}}^q\right) = \mathcal{E}\left(x_1^q | y_{1\mathcal{R}}^q\right) \mathcal{E}\left(x_2^q | y_{2\mathcal{R}}^q\right) = \tanh\left(\frac{LLR_{x_{1,R}^q}}{2}\right) \tanh\left(\frac{LLR_{x_{2,R}^q}}{2}\right), \tag{2.4}$$

where $LLR_{x_{i,\mathcal{R}}^q}$ represents the log-likelihood ratio (LLR) of $y_{i\mathcal{R}}^q$ at the relay, which is calculated as

$$LLR_{x_{i,\mathcal{R}}^q} = \ln \frac{p\left(x_i^q = 1 | h_{i\mathcal{R}}, y_{i\mathcal{R}}^q\right)}{p\left(x_i^q = -1 | h_{i\mathcal{R}}, y_{i\mathcal{R}}^q\right)} = \frac{2\sqrt{E_i} h_{i\mathcal{R}} y_{i\mathcal{R}}^q}{\sigma^2}. \tag{2.5}$$

And the power-normalized relay function $f(y_{1\mathcal{R}}^q, y_{2\mathcal{R}}^q)$ is defined as

$$f_{\mathrm{EF}}(y_{1\mathcal{R}}^q, y_{2\mathcal{R}}^q) = \frac{\tanh\left(\frac{LLR_{x_{1,\mathcal{R}}^q}}{2}\right) \tanh\left(\frac{LLR_{x_{2,\mathcal{R}}^q}}{2}\right)}{\sqrt{\mathcal{E}\left[\left|\tanh\left(\frac{LLR_{x_{1,\mathcal{R}}^q}}{2}\right) \tanh\left(\frac{LLR_{x_{2,\mathcal{R}}^q}}{2}\right)\right|^2\right]}}. \tag{2.6}$$

2.2 Compressive Sensing

The task of processing many kinds of natural signals is often to identify and estimate a few significant coefficients underlying the signals. This is because most of the information of a signal, in a proper basis, resides in just a few large coefficients, while rest of the information can be neglected. The conventional wisdom in data acquisition is that the sensing process first acquires the entire data, then throws away the majority of the small coefficients and only keeps the minority of the significant coefficients [51]. Admittedly, sensing the entire signal while discarding most of the information at a later stage wastes time, energy and resources. At the same time this suggests a proposition that only the information residing in the significant coefficients need to be sensed, instead of sensing the entire data and discarding most of the information at a later stage. To our great interest, the work in [52] already demonstrates that the information within the few significant coefficients can be encoded by a small number of random linear projections. Afterwards authors in [53–55] have proposed possible recovery algorithms to decode the original signals from these random projections, and this ground-breaking research topic is referred to as compressive sensing (CS).

In this section, we will go through the basic encoding techniques of compressive sensing. Specifically, we will briefly discuss several decoding algorithms of CS, including Basis Pursuit via linear programming [56], and one of the many greedy methods, namely Orthogonal Matching Pursuit (OMP) [57]. Moreover, we will give a concrete explanation of belief propagation algorithm under the Bayesian framework crucial to the design in Chapter 3.

2.2.1 Sparsity and Encoding

The basic knowledge of CS is that most of the information included in a signal only rests within a few large coefficients, and this feature is referred to as sparsity. Define a signal vector $\boldsymbol{x} \in \mathbb{R}^l$, if it has the following form

$$\boldsymbol{x} = \boldsymbol{\Psi}\boldsymbol{\theta}, \tag{2.7}$$

where $\boldsymbol{\Psi} \in \mathbb{R}^{l \times l}$ is an orthonormal basis, $\boldsymbol{\theta} \in \mathbb{R}^l$ satisfies $\|\boldsymbol{\theta}\|_0 = k \ll l$, and $\|\cdot\|_0$ denotes the l_0 norm which counts the number of nonzero entries in a vector. For $1 \leq p < \infty$, we

denote by $\|\boldsymbol{x}\|_p$ as the usual norm,

$$\|\boldsymbol{x}\|_p = \left(\sum_{i=1}^{l} |x_i|^p \right)^{\frac{1}{p}}, \tag{2.8}$$

and $\|\boldsymbol{x}\|_\infty = \max |x_i|$.

Then the vector $\boldsymbol{x}$ has sparsity; we also call the signal is k-sparse. If there exists an orthonormal basis $\boldsymbol{\Psi}$, there is no need to sample all of the l elements in the vector $\boldsymbol{x}$; instead, a small number of the linear combinations of the k elements are enough for reconstruction of the signal at the receiver [53, 54]. We obtain a measurement vector $\boldsymbol{y}$ by computing m linear projections of $\boldsymbol{x}$ via an encoding matrix $\boldsymbol{\Phi}$, where $\boldsymbol{\Phi} \in \mathbb{R}^{m \times l}$, and the encoding process can be given by

$$\boldsymbol{y} = \boldsymbol{\Phi}\boldsymbol{x}. \tag{2.9}$$

This is the original definition of sparsity for strictly sparse signal; it means that the signal has non-zero entries and zero entries. Approximately sparse signal models are sequentially explored to broad the application range [58]. In this scenario, signals need to have $k \ll l$ large coefficients, and the rest of the remaining coefficients are only required to be small but not necessarily zero. For compressible signals, if all of the coefficients are sorted, they would decay fast according to the power law, which is given by

$$|x_i^*| \le ci^{(-1/v)}, \tag{2.10}$$

where $\boldsymbol{x}^*$ represents the non-increasing arrangement of the vector $\boldsymbol{x}$, $v \in (0, 1)$, and c is a positive constant.

Besides, in real applications, the measurements are subject to some noise and the imprecision of the sensing devices. Then for the noisy scenario, Eq. (2.9) can be rewritten as

$$\boldsymbol{y} = \boldsymbol{\Phi}\boldsymbol{x} + \boldsymbol{n}, \tag{2.11}$$

where $\boldsymbol{n}$ denotes the noise vector.

2.2.2 Reconstruction Algorithms

Given the observed measurement vector $\boldsymbol{y}$ and the encoding matrix $\boldsymbol{\Phi}$, we aim to decode $\boldsymbol{x}$. Decoding $\boldsymbol{x}$ from Eq. (2.9) is superficially an ill-posed inverse problem, but the sparsity feature underlying $\boldsymbol{x}$ allows recovery from less measurements. In the following, we will describe two commonly used algorithms: the basis pursuit algorithm and the orthogonal matching pursuit algorithm. We also will give a detailed explanation of the compressive sensing via belief propagation (CS-BP) algorithm.

2.2.2.1 Basis Pursuit

To solve an ill-posed inverse problem, optimization comes as a natural idea. It is to implement traversing through all of the sparsest coefficient vectors $\boldsymbol{\theta}$ that satisfy the measurement vector $\boldsymbol{y}$. Once we have sufficient m measurements and a strictly sparse signal $\boldsymbol{x}$, we draw the solution by calculating the l_0 as follows.

$$\hat{\boldsymbol{\theta}} = \arg\min \|\boldsymbol{\theta}\|_0 \quad \text{s.t.} \, \boldsymbol{y} = \boldsymbol{\Phi}\boldsymbol{\Psi}\boldsymbol{\theta}. \tag{2.12}$$

However, it is demonstrated in [59] that solving this l_0 optimization is NP-complete and unstable; it requires an exhaustive search of all of the A_l^k locations of nonzero entries in $\boldsymbol{x}$. Fortunately, an l_1 minimization surprisingly offers a desired outcome [53,54] by solving

$$\hat{\boldsymbol{\theta}} = \arg\min \|\boldsymbol{\theta}\|_1 \quad \text{s.t.} \, \boldsymbol{y} = \boldsymbol{\Phi}\boldsymbol{\Psi}\boldsymbol{\theta}. \tag{2.13}$$

According to Eq. (2.13), an exact reproduction of the k-sparse signal $\boldsymbol{x}$ can be recovered by using only $m = \mathcal{O}\left(k\log\left(l/k\right)\right)$ independent and identically distributed (i.i.d.) Gaussian measurements. Such an optimization problem is referred to as basis pursuit [56], and it can be easily solved via the linear programming technique who has a $\mathcal{O}(l^3)$ cubic computational complexity.

For robust recovery from noisy data in Eq. (2.11), we utilize the l_1 minimization with relaxed

constraints for recovery:

$$\hat{\boldsymbol{\theta}} = \arg\min \|\boldsymbol{\theta}\|_1 \quad \text{s.t.} \|\boldsymbol{\Phi\Psi\theta} - \boldsymbol{y}\|_2 \leq \varepsilon, \tag{2.14}$$

where ε denotes the amount of noise in the data $\boldsymbol{y}$.

2.2.2.2   Orthogonal Matching Pursuit

The large amount of computation in the basic pursuit algorithm consumes a lot of time; this drives researchers to focus on faster decoding algorithms. Greedy algorithms are thus proposed by computing the support of the sparse signal $\boldsymbol{x}$ in an iterative way. As long as the support of $\boldsymbol{x}$ is computed correctly, we can take advantage of the pseudo-inverse of the measurement matrix to recover the actual $\boldsymbol{x}$.

The orthogonal matching pursuit (OMP) algorithm [57] is one branch of many greedy algorithms that help to speed up the CS decoding process. In OMP, we assume that $\boldsymbol{\Phi}$ is a subGaussian encoding matrix, then $\boldsymbol{\Phi}^*\boldsymbol{\Phi}$ is approximate to an identity matrix, where $\boldsymbol{\Phi}^*$ is the conjugate of $\boldsymbol{\Phi}$. Therefore, it is expected that the largest coordinate lying in the measurement vector $\boldsymbol{y}$ corresponds to a non-zero entry of $\boldsymbol{x}$; we can estimate a corresponding coordinate in the measurement $\boldsymbol{y}$ for the support of $\boldsymbol{x}$. Afterwards, this coordinate is eliminated from $\boldsymbol{y}$, with further repeating estimates of other coordinates iteratively, till the entire sequence of $\boldsymbol{x}$ is reconstructed. We briefly summarize the OMP algorithm in algorithm 1.

In total, the OMP algorithm provides a faster CS. It requires the same level of measurements as the basic pursuit algorithm, namely $m = \mathcal{O}\left(k \log\left(l/k\right)\right)$, but a smaller computational complexity, i.e., $\mathcal{O}\left(l\log^2\left(l\right)\right)$.

2.2.2.3   Decoding via Belief Propagation

The reconstruction algorithms listed above are based on a dense encoding matrix, whereas an array of structured matrices have emerged leading to faster decoding. The CS-BP algorithm adopts a sparse encoding matrix $\boldsymbol{\Phi}$ and a belief propagation decoding algorithm to further speed up the encoding and decoding process of compressive sensing [58]. With regard to

---

Algorithm 1: The OMP algorithm

---

1 **begin**

2   Initialize an index set $I = \emptyset$, and a residual vector $\boldsymbol{r} = \boldsymbol{y}$.

3   **for** iteration $= 1 : \mathrm{k}$ **do**

4   Select the largest coordinate λ of $\boldsymbol{u} = \boldsymbol{\Phi}^* \boldsymbol{r}$ in absolute value.

5   Add the chosen coordinate λ into I, namely $I \to I \cup \{\lambda\}$, and update the residual vector by

$$\hat{\boldsymbol{x}} = \arg\min_{\boldsymbol{x}'} \|\boldsymbol{y} - \boldsymbol{\Phi}|_I \boldsymbol{x}'\|_2, \quad \boldsymbol{r} = \boldsymbol{y} - \boldsymbol{\Phi}\boldsymbol{x}' \qquad (2.15)$$

6   **end**

7   Output the support set I, define the pseudo-inverse of $\boldsymbol{\Phi}$ by $\boldsymbol{\Phi}_I^{\dagger} = (\boldsymbol{\Phi}_I^* \boldsymbol{\Phi}_I)^{-1} \boldsymbol{\Phi}_I^*$, and form the estimate vector of $\boldsymbol{x}$ by doing

$$\hat{\boldsymbol{x}} = \boldsymbol{\Phi}_I^{\dagger} \boldsymbol{y}. \qquad (2.16)$$

8 **end**

---

large systems, CS-BP has already been proved asymptotically optimal [60]. A sparse en-
coding matrix is flexible to a variety of signal models, authors in [61] used a sparse matrix
for the special case of noiseless measurement of strictly sparse signals, while in [58] they
managed to apply CS to approximately sparse signals.

In conventional CS, the Shannon's random code constructions shed light on building dense
sub-Gaussian sparse encoding matrices [53, 54]. However, a large amount of computation
underlying a dense encoding matrix is not efficient, as fast encoding and decoding can not
be directly applied. Later on, a sparse encoding matrix is proposed based on the insight of
the low-density parity-check (LDPC) codes [62, 63], as multiplication by a sparse matrix is
fast. A sparse Rademacher LDPC-like matrix is a typical example of sparse matrices with
entries restricted to $\{-1, 0, 1\}$. This enables the computation of multiplication of matrices to
be only the sums and differences of subsets of the vector $\boldsymbol{x}$. The row or column weights of
the encoding matrix $\boldsymbol{\Phi}$ are varied according to the signal model. Generally, the row weight
is chosen on the basis of signal features, such as sparsity. Besides, it is common to fix the
row weight in order to ensure that each row of $\boldsymbol{\Phi}$ contains exactly nonzero entries.

We present the sparse matrix $\boldsymbol{\Phi}$ as a sparse bipartite graph shown in Fig. 2.3; it is in a manner
similar to LDPC channel coding [62, 63]. The sparse feature of the encoding matrix not only
accelerates the encoding and decoding process, but also reduces the number of loops in the
graph, contributing to the convergence of a message passing method. The aim of Eq. (2.9) is
to estimate $\boldsymbol{x}$ provided that the encoding matrix $\boldsymbol{\Phi}$ and the measurement vector $\boldsymbol{y}$ are known.
However, because the length of measurements is shorter than the length of the initial vector,
solving Eq. (2.9) leads to infinite solutions. In CS-BP, the MMSE estimate is considered to
solve the under-determined equation. Let $\boldsymbol{X} = [X(1), \ldots, X(l)]$ be a random vector in $\mathbb{R}^l$
and $\boldsymbol{x} = [x(1), \ldots, x(l)]$ be an outcome of $\boldsymbol{X}$. Then the MMSE estimate can be expressed
as,

$$\hat{\boldsymbol{x}}_{\mathrm{MMSE}} = \arg\min_{\boldsymbol{x}'} \mathcal{E} \left\| \boldsymbol{X} - \boldsymbol{x}' \right\|_2^2 \mathrm{s.t.} \boldsymbol{y} = \boldsymbol{\Phi} \boldsymbol{x}', \tag{2.17}$$

where the expectation is taken on the prior PDF for $\boldsymbol{X}$. Alternatively, the MMSE estimate
can be denoted by the conditional mean,

$$\hat{\boldsymbol{x}}_{\mathrm{MMSE}} = \mathcal{E}[\boldsymbol{X} | \boldsymbol{Y} = \boldsymbol{y}], \tag{2.18}$$

where $\boldsymbol{Y}$ is a random vector in $\mathbb{R}^l$ that can generate the measurement vector $\boldsymbol{y}$.
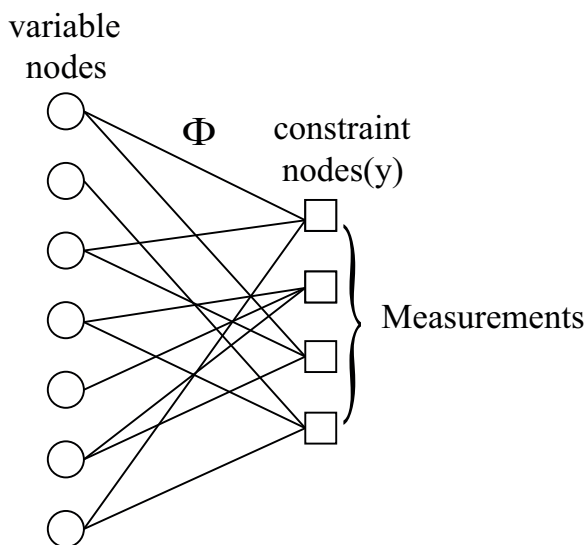
Figure 2.3: Bipartite graph connecting the variables nodes and constraint nodes in belief propagation.

The iterative message passing algorithm over factor graphs becomes a natural means to solving such a problem. In a bipartite graph, the measurement vector $\boldsymbol{y}$ is set to occupy constraint nodes; our goal is to find the MMSE estimates of vector $\boldsymbol{x}$ on the variable nodes side. CS-BP enables message passing between variable nodes and constraint nodes. Based on the obtained measurements, CS-BP approximates the marginal distributions of all the coefficients shown in the factor graph. In Fig. 2.3, we define the set of variable nodes that the cth constraint node n_c depends on by their indices $V(c)$ and the set of constraint nodes that vth variable node n_v depends on by $C(v)$. We introduce $V(c)\backslash v$, $n_c\backslash v$ to represent the set $V(c)$ with variable node n_v excluded and the set of variables in n_c with n_v excluded, respectively. Then we denote the messages sent from the variable nodes to constraint nodes by $q_{v\to c}$ and the messages sent from the constraint nodes to variable nodes by $r_{c\to v}$. The updating principle for the two sets of messages is defined in [64, (26.2)]:

$$q_{v\to c}(n_v) = \prod_{c'\in C(v)\backslash c} r_{c'\to v}(n_v),$$

(2.19)

$$r_{c\to v}(n_v) = \sum_{x_c\backslash v}\left(f_c(n_c)\prod_{v'\in V(c)\backslash v} q_{v'\to c}(n_{v'})\right),$$

(2.20)

where $f_c(n_c)$ is a function of the constraint node n_c that constrains on the set of variable nodes. In CS-BP, the constraint node n_c is a linear combination of n_v, whose weights are

only 1 and -1. When PDFs are being passed along the edges as messages, Eq. (2.20) corresponds to the convolution of the received PDFs at the constraint node. At the variable nodes, Eq. (2.19) corresponds to the multiplication of the PDFs. The marginal distribution, i.e., the PDF of each variable node, is obtained by the multiplication of all the incoming messages linked to this node, which can be written as,

$$p(n_v) = \prod_{c' \in C(v)} r_{c' \to v}(n_v). \tag{2.21}$$

Note that if the noise item exists, e.g. Eq. (2.11), except that the messages passed from variables nodes set $V(c)$ with n_v excluded are convolved at n_c, the PDF of the noise item is further convolved. Besides, because loops and quantization errors exist in the factor graphs, damping methods are applied to stabilizing the decoding process by adding old estimates to new estimates in a proper weight [65]. The CS-BP decoding algorithm is summarized in algorithm 2.

To further increase the computation efficiency of the CS-BP algorithm, point-wise multiplication of messages is performed corresponding to the multiplication of PDFs in Eq. (2.19); the convolution of the messages in Eq. (2.20) is computed in the frequency domain via fast fourier transform (FFT); FFT has already been used in LDPC decoding using BP in [64]. Additionally, modifications to Eq. (2.19) and Eq. (2.20) are performed to reduce computation of the iterations as follows,

$$q_{v \to c}(n_v) = \frac{\displaystyle\prod_{c' \in C(v) \backslash c} r_{c' \to v}(n_v)}{r_{c \to v}(n_v)},$$

$$r_{c \to v}(n_v) = \sum_{x_c \backslash v} \left(f_c(n_c) \frac{\displaystyle\prod_{v' \in V(c) \backslash v} q_{v' \to c}(n_{v'})}{q_{v \to c}(n_{v'})} \right). \tag{2.22}$$

The modifications made in Eq. (2.22) can apparently reduce the computation, as the numerators are only computed once and reused for all of the messages diverging from the certain node.

Overall, the CS-BP algorithm needs $\mathcal{O}(k \log(l))$ measurements and $\mathcal{O}(l \log^2(l))$ computation to decode a signal of length l containing k large coefficients. Besides, the main advan-

---

Algorithm 2: The CS-BP decoding algorithm

---

1 **begin**

2   At the first iteration, set up the data structures with messages $q_{v \to c}(n_v)$ and $r_{c \to v}(n_v)$, initialize messages $q_{v \to c}(n_v)$ with the signal prior PDF.

3   **for** iteration $= 2:$ max **do**

4   For every measurement $c = 1, \ldots, m$, compute $r_{c \to v}(n_v)$ for all of the neighbouring variable nodes $n(c)$ via the convolution defined in Eq. (2.20). If noise exists in Eq. (2.11), do further convolution of the noise PDF. Apply damping methods by weighing new estimates with the old estimates from the previous iteration.

5   For every coefficient $v = 1, \ldots, l$, compute $q_{v \to c}(n_v)$ for all of the neighbouring constraint nodes $n(v)$ via multiplication defined in Eq. (2.19). Apply damping methods by weighing new and old estimates.

6   **end**

7   At each variable node, compute MMSE estimate based on Eq. (2.21) and output the required data.

8 **end**

---

tage of the CS-BP algorithm is that it can be flexibly applied to different prior distributions, as long as the PDF of the transmitted signal can be captured. However, sampling of the PDF requires large memory and introduces quantization errors, which inevitably reduces the precision and becomes a hindrance to the convergence during message passing.

2.3   Trellis coding

The terminology of trellis coding was invented by Gottfried Ungerboeck of IBM in 1982 [66]. It helps to improve error performance without increasing data rate, as channel coding can offer expanded sets of multilevel signals and in turn increases the Euclidean distance. With larger distance between the signal sequences in Euclidean space, the signal waveforms representing these information sequences would be more impervious to the noise-induced detection errors [67].

It is apparent that a length-l sequence needs to be encoded into a set of $2^{(l+1)}$ channel signals for better error performance. This can be easily accomplished by implementing a rate-$l/(l + 1)$ convolution encoder; the convolutional encoder is concatenated with a subsequent modulation scheme, mapping these $(l + 1)$ bits into a larger set of channel signals. This encoding process is shown in Fig. 2.4. We denote by $d(\boldsymbol{a}_n, \boldsymbol{a}'_n)$ the Euclidean distance between the channel signals $\boldsymbol{a}_n$ and $\boldsymbol{a}'_n$; therefore, the encoder is aiming to achieve the maximum free Euclidean distance between all pairs of the channel-signal sequences $\{\boldsymbol{a}_n\}$ and $\{\boldsymbol{a}'_n\}$ that can be produced by the encoder, namely

$$d_{\text{free}} = \min_{\{\boldsymbol{a}_n\} \neq \{\boldsymbol{a}'_n\}} \sqrt{\left[\sum_n d^2 \left(\boldsymbol{a}_n, \boldsymbol{a}'_n \right) \right]}. \tag{2.23}$$

In order to achieve the maximum free Euclidean distance, Ungerboeck introduced a mapping rule called set partitioning in [66]. The underlying principle is that this mapping rule successively partitions a channel signal set into subsets with increasing minimum distances between each signal within the same subset. Fig. 2.5 illustrates how this mapping scheme works with an 8PSK modulation, and it can be applicable to any other modulation scheme. The increased minimum distance after successive partitioning is represented by $\delta_0 < \delta_1 < \delta_2$.
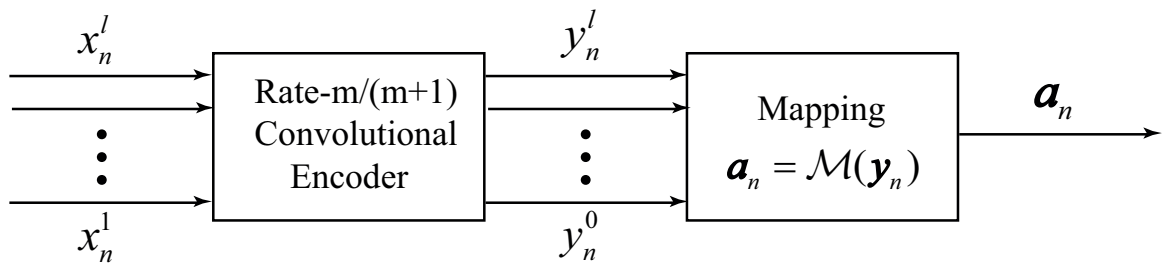
Figure 2.4: Multilevel encoder structure.
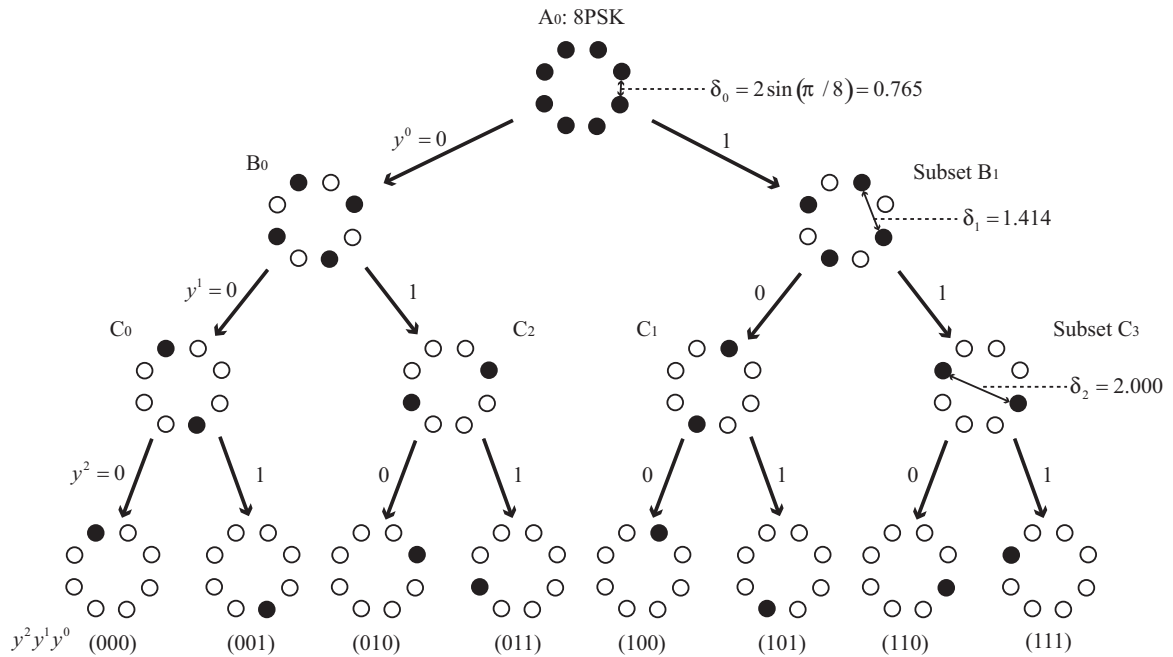
Figure 2.5: Set partitioning of 8PSK channel signals.

The term trellis is formed because the mapping process can be described by a state-transition (trellis) diagram similar to the trellis diagrams of binary convolutional codes. The trellis coding was first introduced as a combined coding and modulation technique in [66], and it can also be viewed as trellis coded modulation [67]. But the branch labeling in TCM differs from convolutional codes, specifically, TCM labels branches with the redundant non-binary modulation signals instead of the binary code symbols.

2.3.1   Trellis Coded Quantization

As mentioned in Chapter 1, trellis coded quantization (TCQ) is involved in delivering soft information from the relay nodes, because it ensures to reduce quantization noise without rate increase by using a structured codebook with an expanded set of quantization levels. TCQ extends the notion of set partitioning and branch labeling of TCM, which enables the trellis coding to prune the expanded set quantization levels down to the reduced rates [68]. A deterministic codebook is then utilized to achieve a computationally simple encoding structure. The Viterbi algorithm (VA) [69, 70] is employed at the encoder, and it is demonstrated that the encoding process only requires 4 multiplications, 4 additions and 4 times of scalar quantization for each source sample, in addition to 2 additions and 1 comparison for each trellis state per source sample [68].

A TCQ encoder works as follows. At an encoding rate R, for each incoming sample, the TCQ maps it into one of the 2^{R+1} reproduction levels (codewords), defined by a finite length of alphabets regarded as the codebook. This codebook is partitioned into 2^R subsets, used as labels on a trellis with 2 branches entering and leaving each trellis state. Usually the TCQ uses a rate $R/(R+1)$ convolutional encoder to define the structure of the trellis, and the Viterbi algorithm is used to search all possible paths in the trellis and select the minimum distortion path. It takes 1 bit to specify the sequence of the trellis branches and $(R-1)$ bits to specify the corresponding codewords in each subset.

Consider two sequences of length l: the input sequence of the source encoder $\boldsymbol{x}$, and the corresponding output sequence $\hat{\boldsymbol{x}}$. The TCQ aims to find the reproduction sequence $\hat{\boldsymbol{x}}$ which has the minimum Euclidean distance with the input sequence. The Euclidean distance between the two sequences is given by

$$d\left(\boldsymbol{x}, \hat{\boldsymbol{x}}\right) = \sqrt{\sum_{i=1}^{l} \left(x_i - \hat{x}_i\right)^2}, \tag{2.24}$$

and the Viterbi algorithm is used to find the output sequence which minimizes $d\left(\boldsymbol{x}, \hat{\boldsymbol{x}}\right)$. Equivalently it can be viewed as minimizing the mean squared error (MSE) of the two sequences, namely

$$\rho_l\left(\boldsymbol{x}, \hat{\boldsymbol{x}}\right) = d^2\left(\boldsymbol{x}, \hat{\boldsymbol{x}}\right)/l. \tag{2.25}$$

We denote by x_k and $\hat{x}_k$ the k-th symbol in the input sequence and the output sequence correspondingly, and we denote by $D_j(s)$ the minimum accumulative squared error distortion for state s at time j, where $s \in \mathcal{S}$ is one of the state in the state space of the trellis. Therefore, $D_{j+1}(s)$ can be recursively calculated by

$$D_{j+1}(s) = \min_{s' \in \mathcal{S}} \left[D_j\left(s'\right) + \left(x_{j+1} - \Lambda\left(s', s\right)\right)^2 \right], \tag{2.26}$$

where $\Lambda\left(s', s\right)$ is the corresponding quantization level assigned to the actually existed transition between the current state s' and the next state s. Denoting by $\mathcal{C}$ the codebook generated from a proper quantizer, we have $\Lambda\left(s', s\right) \in \mathcal{C}$. To solve Eq. (2.26), TCQ starts from $D_0(s) = 0$, $\forall s \in \mathcal{S}$, which means that the TCQ can start at any state. For feasible synchronization at both the encoder and decoder, initialization can be implemented by fixing the start state as s^0, where $s^0 \in \mathcal{S}$, and setting $D_0(s^0) = 0$ and $D_0(s) = \infty$, given $s \neq s^0$, $s \in \mathcal{S}$.

TCQ keeps track of the squared error distortion of the survivor path through the trellis, and finally chooses the survivor path that has the minimum accumulative distortion, namely,

$$D_{\min}(s^l) = \min_{\forall s \in \mathcal{S}} D_l(s), \tag{2.27}$$

where s^l represents the final state in the trellis. Then TCQ tracks back from the final state to the initial state and thus finds the survivor path with the minimum squared error distortion.

An example of a TCQ encoder for memoryless Gaussian source at rate $R = 1$ bit/sample is given below.

- The Gaussian source generates the sequence $\boldsymbol{x}$ consisting of $l = 1000$ symbols, $\boldsymbol{x} = (-0.9818, 0.0057, -0.2679, -0.5454, 1.2585, 0.4240, \dots, -1.8464, -1.2401)$.

- With a rate $(R + 1)$ Lloyd-Max quantizer [71, 72], the corresponding codebook of the input sequence is give by $\mathcal{C} = (c_1, c_2, c_3, c_4) = (-1.3308, -0.2639, 0.6424, 1.7734)$.

- A proper convolutional encoder, e.g. a rate-1/2 $(5, 2)$ encoder, defines the trellis, branches of which are labeled with codewords c_i, $i = \{1, 2, 3, 4\}$, as shown in Fig. 2.6.

- Viterbi Algorithm is used to encode the input sequence $\boldsymbol{x}$ as show in Fig. 2.7. The
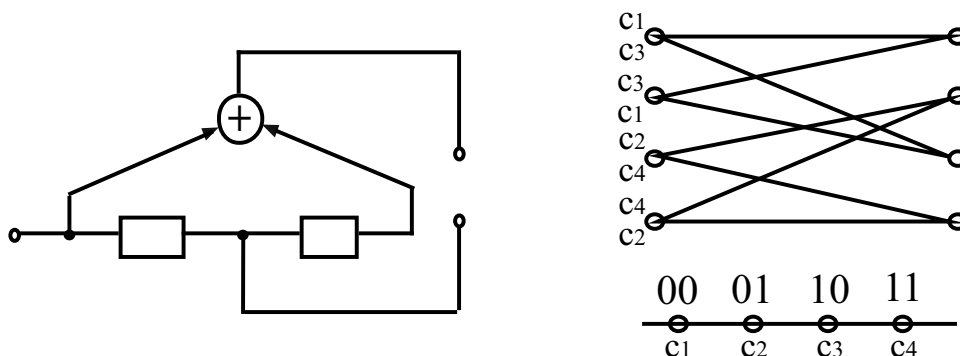
Figure 2.6: A rate-1/2 convolutional encoder and corresponding trellis branch labeling.
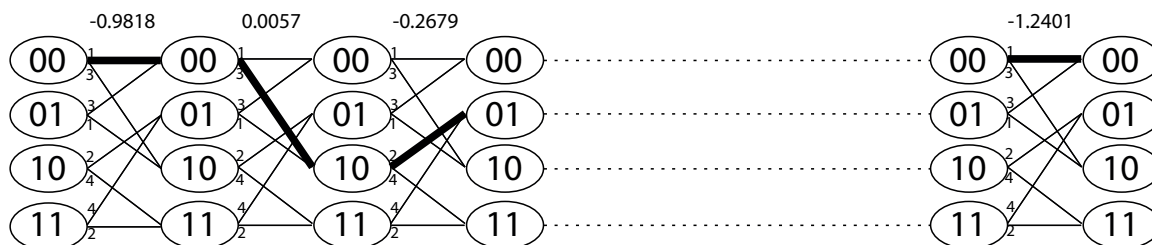
Figure 2.7: Viterbi Algorithm for source encoding at rate 1 with a 4 state trellis

.

solid line depicted in Fig. 2.7 is the survivor path which has the minimum Euclidean distance to the source sequence x.

2.3.2 Joint Trellis Coded Quantization/Modulation

Joint trellis coded quantization/modulation is one means of joint source/channel coding techniques. In the joint trellis coded quantization/modulation (TCQ/M) system, the encoding rate for the TCQ and the transmission rate for the TCM are the same. They both use the identical trellis to ensure the consistent labeling in the trellis diagram; this can guarantee that likely channel error events will only lead to small additional TCQ distortion [73]. Both the TCQ and the TCM use the Viterbi algorithm to find the appropriate sequence path of quantization levels or modulation symbols that have the shortest Euclidean distance to the corresponding input.

The TCQ/M system functions as follows. The quantization process is first adopted as de-

scribed in Section 2.3.1. Combined with the TCM, the single bit used in the TCQ is then taken as the input to the TCM convolutional encoder, and the rest $(R-1)$ bits are used to specify the modulation symbol in the TCM subset. As the TCQ generates a sequence consisting of the 2^{R+1} reproduction levels from the defined codebook, these levels are mapped to the symbols made up of the 2^{R+1}-point TCM alphabets [68, 73, 74].

2.3.3 Decoding

The Viterbi Algorithm (VA) can be used to decode the TCM signals. The output sequence is formed as the one that has the minimum Euclidean distance from the received signals. Then the decoded bits are simply obtained from the trellis branch specified by the 1 bit and the decoded symbols specified by the $(R-1)$ bits. For the decoding of TCQ, the Viterbi algorithm uses the 1 bit to specify the trellis branch and the rest $(R-1)$ bits to specify the codeword in the corresponding subset, and then outputs this codeword. Below is a detailed description of the Viterbi algorithm.

2.3.3.1 The Viterbi Algorithm

The VA is accomplished by performing the maximum likelihood decoding of convolutional codes. It involves a search through the trellis for the most likely sequence. For an (n, k) convolutional code, its trellis diagram has 2^k branches entering and leaving each state.

Assume that the information sequence $\boldsymbol{x}$ is encoded by an (n, k) convolutional code into a codeword $\boldsymbol{c} = (\boldsymbol{c}_1, \boldsymbol{c}_2, \cdots, \boldsymbol{c}_{l+m})$ of length $(l + m)$, where $\boldsymbol{c}_i = (c_{i,1}, \cdots, c_{i,n})$, and that the received sequence is denoted by $\boldsymbol{y} = (\boldsymbol{y}_1, \boldsymbol{y}_2, \cdots, \boldsymbol{y}_{l+m})$. A maximum likelihood decoder is performed based on the received sequence to choose the survival path $\hat{\boldsymbol{c}}$. The aim is to maximize the log-likelihood function of $\log p(\boldsymbol{y} \mid \hat{\boldsymbol{c}})$. The conditional PDF $p(\boldsymbol{y} \mid \hat{\boldsymbol{c}})$ is given by

$$p(\boldsymbol{y} \mid \hat{\boldsymbol{c}}) = \prod_{i=1}^{l+m} p(\boldsymbol{y}_i \mid \hat{\boldsymbol{c}}_i), \tag{2.28}$$

which is equivalent to

$$\log p(\boldsymbol{y} \mid \hat{\boldsymbol{c}}) = \sum_{i=1}^{l+m} \log p(\boldsymbol{y}_i \mid \hat{\boldsymbol{c}}_i), \tag{2.29}$$

where $\log p(\boldsymbol{y} \mid \hat{\boldsymbol{c}})$ denotes the path metric and $\log p(\boldsymbol{y}_i \mid \hat{\boldsymbol{c}}_i)$ represents the branch metric for the i-th branch.

The Viterbi algorithm is then to select the survivor by comparing the metrics of all paths merging into each state and storing the path with the largest metric, as well as its own metric. Finally the survivor is decoded. The Viterbi algorithm is summarized in algorithm 3.

Algorithm 3: The Viterbi algorithm

---

1 **begin**

2   At time $t = 1$, compute the branch metric for the single branch merging into each state. Store the branch metric (the survivor) and its own metric for each state.

3   **for** $t = 2 \colon l + m$ **do**

4   Obtain the partial metric for each path entering a state by adding the branch metric entering that state to the metric of the connecting survivor at the preceding trellis depth. For each state, store the path with the largest metric (the survivor), along with its metric, and eliminate all other paths.

5   **end**

6   Keep the final survivor and decode the code sequence.

7 **end**

In terms of the branch metrics, for convolutional codes, they are Hamming distance and squared Euclidean distance for hard and soft decoding, respectively.

Chapter 3

Compressive Soft Forwarding in Network Coded Multiple Access Relay Channels

In this chapter, we design a novel EF protocol in MARC where two correlated sources transmit their information to the common destination with the help of a relay. With the application of network coding at the relay, the network coded soft symbols contain redundant information due to the correlated sources; the redundancy can be compressed before soft symbols being forwarded. Specifically, we first derive the value of the network coded soft symbol by considering the correlation of the two sources. Due to this correlation, the values of the majority of soft symbols are close to the area of one. Then we convert the network coded soft symbol vector into a sparse vector; such a sparse vector is suitable for compression by using CS. Next, we analyze the performance of the proposed EF protocol by comparing the soft symbol value and received signal-to-noise ratio with the conventional EF protocol. Simulations show that our protocol can achieve the same BER as the conventional EF protocol with proper compression rates, while it consumes much less transmission time due to the compression.

3.1 Introduction

WSN serve as a much more feasible means than the conventional wired sensing network, given the features of its low-cost and low-power sensor nodes [13]. In the case where neighboring sensor nodes obtain spatially correlated measurements, the topic of the sensor reachback problem, specifically, how to efficiently transmit correlated data from multiple source nodes to one or multiple destination nodes, has drawn attention from the academia recently [32].

On the other hand, in order to further enhance transmission efficiency, support long distance transmission and combat fading channels, relay nodes are introduced into WSN. These relay nodes are relatively costly, but more powerful [14]. They listen to the signals transmitted by the source nodes, implement signal processing on the received signal, and further forward the processed signal to the destination. Therefore, the destination nodes can exploit spatial diversity by combining signals from both the source nodes and the relay nodes. One specific scenario is that one relay assists multiple sources, which is modeled by the MARC. In the case of independent sources, quite a few relay strategies have been explored [25, 28, 38, 75–78].

However, none of these works considered correlated sources. In this work, we consider an MARC system with correlated sources. Upon deriving the expression of the network coded soft symbol at the relay from two correlated sources, we obtain sparsity from the processed signals by doing proper transformation on the soft symbol vector. Therefore, it becomes desirable to exploit this sparsity, in order that the relay node can use less transmission time. The ground-breaking work in CS has recently proved that a sparse vector can be effectively recovered from a small number of random projections onto a proper basis [53, 54, 58]. In the literature, works on CS applied in WSN have emerged recently [79, 80]. The novel form of NC approach named Netcompress in [79] has been proved to meet the reconstruction condition of CS and overcome the high link-failure rate in WSN, and experimental proof supports that Netcompress approach only needs half the number of nodes packets to obtain reasonable recovery. In [80], the authors have proposed a coding scheme on a finite field based on the quantized measures in WSN, and this coding scheme coincides with the Bayesian BP structure in [58] with a nonbinary parity-check encoding matrix and the BP decoding algorithm.

In this chapter, we investigate the SIF protocols in the MARC with NC and correlated sources. We consider to use CS [54, 58] to compress and forward the network coded soft information at the relay. Specifically, we design a novel EF based SIF protocol by compressing the soft network coded symbols at the relay with CS, which is referred to as correlated EF with CS. We first study the network coded soft symbol in the MARC with the correlated sources. Due to the correlation of the two sources, the values of the majority of the soft symbols are close to the area of one. Then we convert the network coded soft symbol vector into a sparse vector to make it suitable to be compressed by the CS. Next, we analyze the performance of the CEF-CS protocol by comparing the soft symbol value and the received SNR with the conventional EF protocol. Simulations show that our CEF-CS protocol can achieve the same BER as the EF protocol with some proper compression rate, while it consumes much less transmission time due to the compression.

The contribution of [58] is that they perform asymptotically optimal Bayesian inference using BP decoding and achieve fast computation. Its theoretical contribution is the derivation of the measurements and decoding complexity. On the other hand, I take advantage of their CS via BP decoding concept and apply it to the network coded symbol vector in the MARC. The original contribution of my thesis lies in the application of CS to the relay model, and my theoretical analyses part in this chapter is about deriving the network coded symbol of the correlated sources, and the reliability comparison between the network coded symbols formed with or without the side information of source correlation.

3.2   System Model

Consider an MARC with two correlated sources, one relay and one destination as shown in Fig. 2.2, where the two sources $\mathcal{S}_1$ and $\mathcal{S}_2$ broadcast their messages to the common destination $\mathcal{D}$ with the help of a half-duplex relay $\mathcal{R}$. Each transmission period consists of three phases. In the first phase, $\mathcal{S}_1$ broadcasts its message, and in the second phase, $\mathcal{S}_2$ broadcasts its message, to the relay and the destination. After the first two phases, the relay processes the network coded information based on the signals from the two sources, which is then forwarded to the destination during the third phase. At the end of each transmission period, the destination decodes the messages of the two sources based on the signals from the sources and the relay.

We denote by $h_{i\mathcal{R}}$, $i = 1, 2$, $h_{i\mathcal{D}}$, and $h_{\mathcal{R}\mathcal{D}}$ the channel coefficients between $\mathcal{S}_i$ and $\mathcal{R}$, between $\mathcal{S}_i$ and $\mathcal{D}$, and between $\mathcal{R}$ and $\mathcal{D}$, respectively, as shown in Fig. 2.2, and denote by $d_{i\mathcal{R}}$, $d_{i\mathcal{D}}$, and $d_{\mathcal{R}\mathcal{D}}$ the distances between $\mathcal{S}_i$ and $\mathcal{R}$, between $\mathcal{S}_i$ and $\mathcal{D}$, and between $\mathcal{R}$ and $\mathcal{D}$, respectively. We assume that $h_{i\mathcal{R}}$, $h_{i\mathcal{D}}$, and $h_{\mathcal{R}\mathcal{D}}$ are independent and identically Rayleigh distributed with the channel gains as $\lambda_{i\mathcal{R}}$, $\lambda_{i\mathcal{D}}$, and $\lambda_{\mathcal{R}\mathcal{D}}$, respectively. These channel gains are related to the corresponding distances with the attenuation exponent γ, i.e., $\lambda_{i\mathcal{R}} = 1/(d_{i\mathcal{R}})^\gamma$, $\lambda_{i\mathcal{D}} = 1/(d_{i\mathcal{D}})^\gamma$, and $\lambda_{\mathcal{R}\mathcal{D}} = 1/(d_{\mathcal{R}\mathcal{D}})^\gamma$. We consider quasi-static fading channels, i.e., the channel coefficients are constant during one transmission period, and change independently from one period to another.

In each transmission period, we assume that each source transmits l *i.i.d.* BPSK symbols. Thus, the symbol vector of $\mathcal{S}_i$ is denoted by $\boldsymbol{x}_i = (x_i^1, \cdots, x_i^l)^T$, $x_i^q \in \{\pm 1\}$ and $q \in \{1, \cdots, l\}$, with the power E_i. The received signals at the relay and at the destination from $\mathcal{S}_i$ can be expressed as

$$\boldsymbol{y}_{i\mathcal{R}} = h_{i\mathcal{R}} \sqrt{E_i} \boldsymbol{x}_i + \boldsymbol{n}_{i\mathcal{R}},$$

$$\boldsymbol{y}_{i\mathcal{D}} = h_{i\mathcal{D}} \sqrt{E_i} \boldsymbol{x}_i + \boldsymbol{n}_{i\mathcal{D}}, \tag{3.1}$$

respectively, where the vectors $\boldsymbol{y}_{i\mathcal{R}}$ and $\boldsymbol{y}_{i\mathcal{D}}$ consist of l received signals, i.e., $\boldsymbol{y}_{i\mathcal{R}} = (y_{i\mathcal{R}}^1, \cdots, y_{i\mathcal{R}}^l)^T$ and $\boldsymbol{y}_{i\mathcal{D}} = (y_{i\mathcal{D}}^1, \cdots, y_{i\mathcal{D}}^l)^T$, the vector $\boldsymbol{n}_{i\mathcal{R}} = (n_{i\mathcal{R}}^1, \cdots, n_{i\mathcal{R}}^l)^T$ consists of l additive white Gaussian noise (AWGN) samples at the relay, and the vector, $\boldsymbol{n}_{i\mathcal{D}} = (n_{i\mathcal{D}}^1, \cdots, n_{i\mathcal{D}}^l)^T$, consists of l AWGN samples at the destination. We assume that all the noise samples at the relay and destination are *i.i.d.* Gaussian variables with a mean zero and variance σ^2, and the sources' power satisfies $E_1 = E_2 = E_\mathcal{S}$. We define the SNR as $\rho \triangleq E_\mathcal{S}/\sigma^2$.

After receiving $\boldsymbol{y}_{i\mathcal{R}}$, the relay detects $\boldsymbol{x}_i$ and obtains the network coded symbol vector as $\boldsymbol{x}_\mathcal{R} = (x_\mathcal{R}^1, \cdots, x_\mathcal{R}^l)^T$, $x_\mathcal{R}^q \in \{\pm 1\}$. A network coded symbol $x_\mathcal{R}^q$ in $\boldsymbol{x}_\mathcal{R}$ can be calculated as $x_\mathcal{R}^q = x_1^q x_2^q$. However, in our CEF-CS protocol, the relay does not forward $\boldsymbol{x}_\mathcal{R}$ directly. Instead, it first obtains the soft symbol of $x_\mathcal{R}^q$ in $\boldsymbol{x}_\mathcal{R}$, denoted by $\tilde{x}_\mathcal{R}^q$. Note that the soft symbol of $x_\mathcal{R}^q$ is equivalent to the expectation of $x_\mathcal{R}^q$ given the received signals, i.e., $\tilde{x}_\mathcal{R}^q = \mathcal{E}[x_\mathcal{R}^q | y_{1\mathcal{R}}^q, y_{2\mathcal{R}}^q]$ [27]. Then the relay compresses the soft symbol vector $\tilde{\boldsymbol{x}}_\mathcal{R} = (\tilde{x}_\mathcal{R}^1, \cdots, \tilde{x}_\mathcal{R}^l)^T$ by exploiting the correlation between the two sources, which will be discussed in detail in the next section. We denote by $\mathcal{B}(\tilde{\boldsymbol{x}}_\mathcal{R})$ the power-normalized vector after compression. The length of $\mathcal{B}(\tilde{\boldsymbol{x}}_\mathcal{R})$, denoted by m, ($m < l$), varies according to different compression rates.

Then the received signal vector at the destination in the third phase can be expressed as

$$\boldsymbol{y}_{\mathcal{RD}} = h_{\mathcal{RD}}\sqrt{E_{\mathcal{R}}}\mathcal{B}(\tilde{\boldsymbol{x}}_{\mathcal{R}}) + \boldsymbol{n}_{\mathcal{RD}}, \qquad (3.2)$$

where $E_{\mathcal{R}}$ is the power at the relay, $\boldsymbol{y}_{\mathcal{RD}} = (y_{\mathcal{RD}}^1, \cdots, y_{\mathcal{RD}}^m)^T$ is the received signal vector, and $\boldsymbol{n}_{\mathcal{RD}} = (n_{\mathcal{RD}}^1, \cdots, n_{\mathcal{RD}}^m)^T$ is the AWGN vector at the destination.

At the end of the third phase, the destination first recovers $\tilde{\boldsymbol{x}}_{\mathcal{R}}$ from $\boldsymbol{y}_{\mathcal{RD}}$; the recovered signals are then combined with the signals from the source-to-destination channels to make hard decisions.

With regard to the modulation schemes, for the signals transmitted from the source nodes to the relay nodes and the destination nodes, BPSK and QPSK modulation schemes are the same because decoding is performed both on the bit level. To my best knowledge, I have not found related works on the high level modulations (beyond QPSK) being applied to the soft information relaying. In addition, as I consider a wireless sensor network, it will be quite challenging if high level modulations are applied to a large number of sensor nodes with low transmission power. The resulting cost will be much increased to implement more complicated modulation schemes over each sensor node.

3.3 Correlated EF with Compressive Sensing

In this section, we introduce our CEF-CS protocol. First, we derive the network coded soft symbols based on the correlated messages from the two sources. We note that the correlated messages from the two sources lead to redundancy in the soft symbol vector $\tilde{\boldsymbol{x}}_{\mathcal{R}}$ at the relay. Then we compress $\tilde{\boldsymbol{x}}_{\mathcal{R}}$ by using compressive sensing.

3.3.1 Network Coded Soft Symbols with Correlated Sources

The correlation between the sources is modeled as follows [81]. Let Z_q, $q = 1, \cdots, l$, be an *i.i.d.* binary random variable with $\Pr(Z_q = 0) = \tau$, where $\tau \in [0, 1]$. Without a loss of generality, we focus on the q-th symbol x_i^q in $\boldsymbol{x}_i$. We define the correlation between x_1^q and

x_2^q as follows. If $Z_q = 0$, then x_1^q and x_2^q are independent, and if $Z_q = 1$, then x_1^q and x_2^q are identical. To simplify the derivation of the network coded soft symbol, we further define the correlation coefficient between x_1^q and x_2^q by $\zeta(x_1^q, x_2^q)$, which can be expressed as

$$\zeta(x_1^q, x_2^q) = \begin{cases} \frac{2-\tau}{4}, & \text{if } x_1^q = 1, x_2^q = 1 \text{ or } x_1^q = -1, x_2^q = -1, \\ \frac{\tau}{4}, & \text{if } x_1^q = 1, x_2^q = -1 \text{ or } x_1^q = -1, x_2^q = 1. \end{cases} \tag{3.3}$$

Based on $\zeta(x_1^q, x_2^q)$, we now derive the soft symbol $\tilde{x}_{\mathcal{R}}^q = \mathcal{E}[x_{\mathcal{R}}^q | y_{1\mathcal{R}}^q, y_{2\mathcal{R}}^q]$, and we have

$$\begin{aligned}
\mathcal{E}[x_{\mathcal{R}}^q | y_{1\mathcal{R}}^q, y_{2\mathcal{R}}^q] &= \sum_{x_1^q = \pm 1, x_2^q = \pm 1} x_1^q x_2^q p\left(x_1^q, x_2^q | y_{1\mathcal{R}}^q, y_{2\mathcal{R}}^q\right) \\
&= \sum_{x_1^q = \pm 1, x_2^q = \pm 1} x_1^q x_2^q \frac{p\left(x_1^q, x_2^q, y_{1\mathcal{R}}^q, y_{2\mathcal{R}}^q\right)}{p\left(y_{1\mathcal{R}}^q, y_{2\mathcal{R}}^q\right)} \\
&= \sum_{x_1^q = \pm 1, x_2^q = \pm 1} x_1^q x_2^q \frac{p\left(y_{1\mathcal{R}}^q, y_{2\mathcal{R}}^q | x_1^q, x_2^q\right) \zeta\left(x_1^q, x_2^q\right)}{\sum_{u = \pm 1, v = \pm 1} p\left(y_{1\mathcal{R}}^q, y_{2\mathcal{R}}^q | u, v\right) \zeta(u, v)} \\
&= \sum_{x_1^q = \pm 1, x_2^q = \pm 1} x_1^q x_2^q \frac{p\left(y_{1\mathcal{R}}^q | x_1^q\right) p\left(y_{2\mathcal{R}}^q | x_2^q\right) \zeta\left(x_1^q, x_2^q\right)}{\sum_{u = \pm 1, v = \pm 1} p\left(y_{1\mathcal{R}}^q | u\right) p\left(y_{2\mathcal{R}}^q | v\right) \zeta(u, v)},
\end{aligned} \tag{3.4}$$

where $p(\cdot)$ denotes the probability density function, and $p\left(y_{i\mathcal{R}}^q | x_i^q\right)$ is conditionally Gaussian distributed, which is expressed as

$$p\left(y_{i\mathcal{R}}^q | x_i^q\right) = \frac{1}{\sqrt{2\pi}\sigma} \exp\left(-\frac{(y_{i\mathcal{R}}^q - h_{i\mathcal{R}} x_i^q)^2}{2\sigma^2}\right). \tag{3.5}$$

3.3.2 Compressive Sensing on Soft Symbol Vector

The correlation between the two sources leads to redundancy in the soft symbol vector $\tilde{\boldsymbol{x}}_{\mathcal{R}}$. By taking the advantage of this redundancy, we can convert $\tilde{\boldsymbol{x}}_{\mathcal{R}}$ to a sparse vector. To show this sparsity, we first investigate the PDF of a network coded soft symbol $\tilde{x}_{\mathcal{R}}^q$. Fig. 3.1 plots the histogram results of a soft symbol vector $\tilde{\boldsymbol{x}}_{\mathcal{R}}$ with τ in Eq. (3.3) equal to 0.2, vector length $l = 10,000$, $h_{1\mathcal{R}} = 0.5$, and $h_{2\mathcal{R}} = 1$. We focus on the curves for the CEF-CS protocol, and consider the SNR $\rho = 0$ dB, 10 dB, and 25 dB (the curve 'EF, SNR=0dB' will be discussed later). We can see that the soft symbols are within the range from -1 to 1. When SNR is
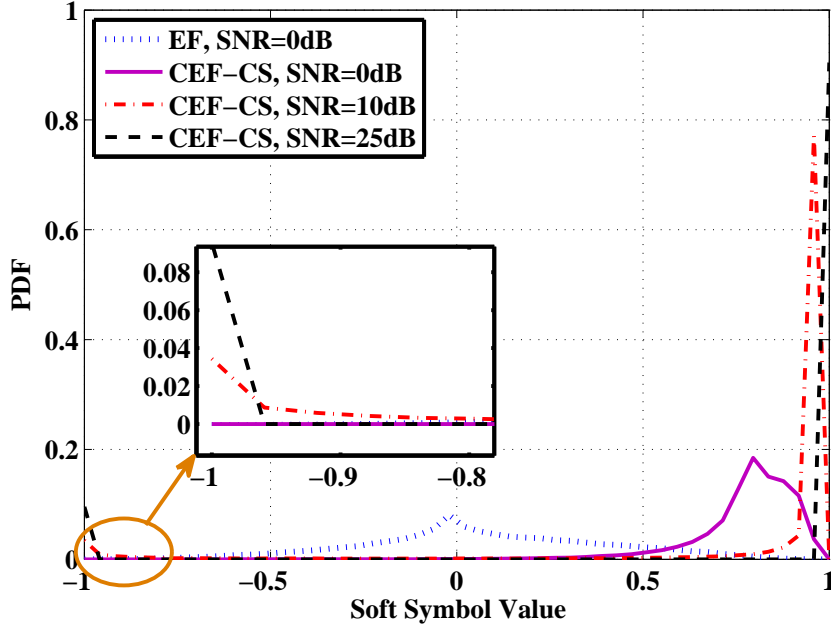
Figure 3.1: The PDF of a soft symbol vector with $\tau = 0.2$, $l = 10,000$, $h_{1\mathcal{R}} = 0.5$, and $h_{2\mathcal{R}} = 1$.

large, the soft symbols are polarized around the areas close to -1 and 1. Furthermore, due to the correlation between the two sources, the majority of the soft symbols are close to 1.

Then we obtain another length-l vector $\tilde{\boldsymbol{x}}'_{\mathcal{R}}$ by calculating $\tilde{\boldsymbol{x}}'_{\mathcal{R}} = \tilde{\boldsymbol{x}}_{\mathcal{R}} - 1$. Obviously, the elements in $\tilde{\boldsymbol{x}}'_{\mathcal{R}}$ are polarized around the areas close to -2 and 0, and the majority of the elements are close to 0. Therefore, the vector $\tilde{\boldsymbol{x}}'_{\mathcal{R}}$ can be viewed as a sparse vector, and such a sparse vector can be compressed by using compressive sensing [58]. We now connect the sparsity in $\tilde{\boldsymbol{x}}'_{\mathcal{R}}$ with τ. We can obtain that when ρ is large enough, there are $(1 - \frac{\tau}{2})l$ elements in $\tilde{\boldsymbol{x}}'_{\mathcal{R}}$ around zeros and $\frac{\tau l}{2}$ elements around -2. Therefore, the sparsity of the vector $\tilde{\boldsymbol{x}}'_{\mathcal{R}}$ is $\frac{\tau}{2}$.

Based on the sparsity of $\tilde{\boldsymbol{x}}'_{\mathcal{R}}$, we encode $\tilde{\boldsymbol{x}}'_{\mathcal{R}}$ with an $m \times l$ $(m < l)$ sparse matrix $\boldsymbol{\Phi}$ composed only of the entries $\{1, -1, 0\}$. Specifically, we select $\boldsymbol{\Phi}$ as a Rademacher encoding matrix according to [58]. For each element ϕ in $\boldsymbol{\Phi}$, we have

$$\phi = \begin{cases} +1, & \text{with probability } \frac{2}{\tau l} \\ 0, & \text{with probability } 1 - \frac{4}{\tau l} \\ -1, & \text{with probability } \frac{2}{\tau l} \end{cases} \quad . \qquad (3.6)$$

The encoded vector $\mathbf{\Phi}\tilde{\boldsymbol{x}}'_{\mathcal{R}}$, or called measurement vector, is of length m. Thus, by transmitting $\mathbf{\Phi}\tilde{\boldsymbol{x}}'_{\mathcal{R}}$ rather than $\tilde{\boldsymbol{x}}_{\mathcal{R}}$, the relay can save $(l-m)$ time slots. The vector $\mathcal{B}(\tilde{\boldsymbol{x}}_{\mathcal{R}})$ in Eq. (3.2) is written as

$$\mathcal{B}(\tilde{\boldsymbol{x}}_{\mathcal{R}}) = \frac{\mathbf{\Phi}\tilde{\boldsymbol{x}}'_{\mathcal{R}}}{\sqrt{\mathcal{E}\left[|\mathbf{\Phi}\tilde{\boldsymbol{x}}'_{\mathcal{R}}|^2\right]}}\sqrt{\frac{l}{m}}. \tag{3.7}$$

Note that the term $\sqrt{l/m}$ in Eq. (3.7) is included to keep relay's transmission power constant during the third phase, since the relay consumes less transmission time slots by compressing $\tilde{\boldsymbol{x}}_{\mathcal{R}}$.

From Fig. 3.1, we can approximate the distribution of $\tilde{\boldsymbol{x}}'_{\mathcal{R}}$ as a mixture of two Gaussian variables with two different mean values and the same variance. This approximation can be equivalently treated as a two-state Gaussian mixture model described in [58] which requires $m = \mathcal{O}\left(\frac{l\tau}{2}\log(l)\right)$ to guarantee the reconstruction. Thus, we need $\mathcal{O}\left(\frac{l\tau}{2}\log(l)\right)$ measurements to recover $\tilde{\boldsymbol{x}}'_{\mathcal{R}}$.

3.3.3 Reconstruction via Belief Propagation

At the destination, the belief propagation (BP) algorithm is applied to recovering $\tilde{\boldsymbol{x}}'_{\mathcal{R}}$, which is of length l. We assume the PDFs of the soft symbol vector at different SNRs are known to the destination, which are used as the prior knowledge for BP [58]. We denote by $\hat{\tilde{\boldsymbol{x}}}'_{\mathcal{R}}$ the recovered $\tilde{\boldsymbol{x}}'_{\mathcal{R}}$ from BP algorithm at the destination. It is easy to recover the network coded soft symbol vector $\tilde{\boldsymbol{x}}_{\mathcal{R}}$, denoted by $\hat{\tilde{\boldsymbol{x}}}_{\mathcal{R}}$, from $\hat{\tilde{\boldsymbol{x}}}'_{\mathcal{R}}$ by calculating $\hat{\tilde{\boldsymbol{x}}}_{\mathcal{R}} = \hat{\tilde{\boldsymbol{x}}}'_{\mathcal{R}} + 1$. Then the recovered soft symbol vector $\hat{\tilde{\boldsymbol{x}}}_{\mathcal{R}}$ will be combined with the signals from the source-to-destination channels to make final decisions on the sources' messages. In the following, we focus on how to obtain $\hat{\tilde{\boldsymbol{x}}}_{\mathcal{R}}$ from the received signal $\boldsymbol{y}_{\mathcal{RD}}$ by using BP.

To make the received signal $\boldsymbol{y}_{\mathcal{RD}}$ suitable for BP process, we first define

$$\beta = \sqrt{\frac{lE_{\mathcal{R}}}{m\mathcal{E}\left[|\mathbf{\Phi}\tilde{\boldsymbol{x}}'_{\mathcal{R}}|^2\right]}}, \tag{3.8}$$

and we have $\boldsymbol{y}_{\mathcal{RD}} = \beta h_{\mathcal{RD}}\mathbf{\Phi}\tilde{\boldsymbol{x}}'_{\mathcal{R}} + \boldsymbol{n}_{\mathcal{RD}}$. Then we obtain a new vector $\boldsymbol{y}$ by calculating $\boldsymbol{y} = \boldsymbol{y}_{\mathcal{RD}}/(\beta h_{\mathcal{RD}})$, i.e., $\boldsymbol{y} = \mathbf{\Phi}\tilde{\boldsymbol{x}}'_{\mathcal{R}} + \boldsymbol{n}$, where $\boldsymbol{n} = \boldsymbol{n}_{\mathcal{RD}}/(\beta h_{\mathcal{RD}})$. The vector $\boldsymbol{y}$ can
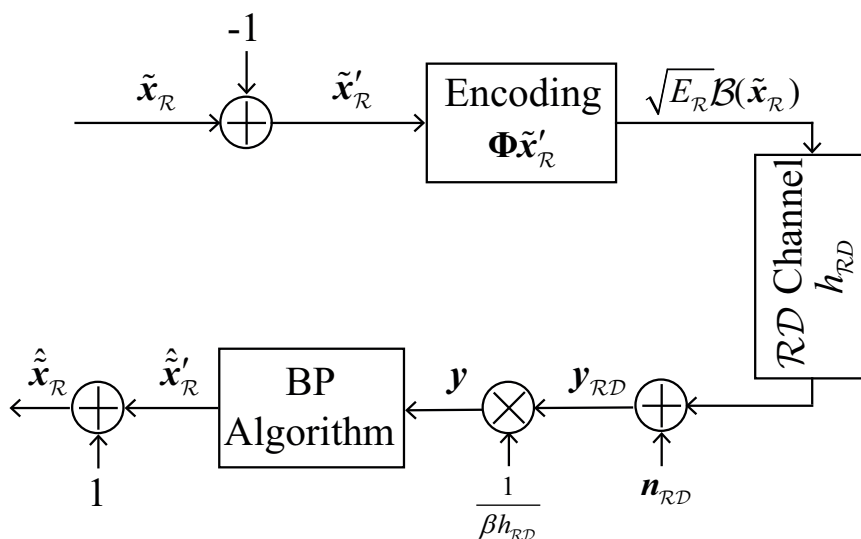
Figure 3.2: The compression and reconstruction process of $\tilde{\boldsymbol{x}}_{\mathcal{R}}$ by using compressive sensing.

be interpreted as the encoded vector $\boldsymbol{\Phi}\tilde{\boldsymbol{x}}_{\mathcal{R}}'$ plus Gaussian noise. We use $\boldsymbol{y}$ as the input of the BP algorithm to recover $\tilde{\boldsymbol{x}}_{\mathcal{R}}'$ as in [58]. After we obtain $\hat{\tilde{\boldsymbol{x}}}_{\mathcal{R}}'$, we can thus obtain $\hat{\tilde{\boldsymbol{x}}}_{\mathcal{R}}$. The compression and reconstruction process of the network coded soft symbol vector $\tilde{\boldsymbol{x}}_{\mathcal{R}}$ is shown in Fig. 3.2.

3.4 Performance Analysis and Comparison

We analyze the soft symbol value and the received SNR at the destination in our CEF-CS protocol, and compare them with the conventional EF protocol [27].

3.4.1 Soft Symbol Value

Recall that the soft symbol $x_{\mathcal{R}}^q$ of our CEF-CS protocol is derived in Eq. (3.4). However, in the conventional EF protocol, the soft symbol is calculated as shown in Eq. (2.4), thus we obtain

$$\tilde{x}_{\mathcal{R}}^q = \tanh\left(\frac{LLR_{x_1^q}}{2}\right) \tanh\left(\frac{LLR_{x_2^q}}{2}\right). \tag{3.9}$$

In fact, the calculation of $\tilde{x}_{\mathcal{R}}^q$ in Eq. (3.9) does not consider the correlation between the two sources.

By comparing the values of $\tilde{x}_{\mathcal{R}}^q$ calculated from Eq. (3.4) and Eq. (3.9), we have the following theorem.

Theorem 1. *The soft symbol calculated by the CEF-CS in Eq. (3.4) has a higher reliability than that calculated by the conventional EF in Eq. (3.9).*

Proof. Please refer to Appendix A.1. □

From the proof of *Theorem 1*, we can see that the CEF-CS considers the correlation of the two sources when calculating $\tilde{x}_{\mathcal{R}}^q$, thus having a higher reliability. Therefore, the CEF-CS always has a better performance than the conventional EF.

In Fig. 3.1, we compare the probability distributions of the network coded soft symbols in the CEF-CS protocol and the EF protocol when $\rho = 0$ dB. It can be seen that with the correlation knowledge exploited by the CEF-CS protocol at the relay, more soft symbols than those in the EF protocol approach the value of 1. In fact, due to the correlation between the two sources, the majority of the network coded symbols calculated in the CEF-CS protocol are 1. Therefore, the soft symbols in the CEF-CS have higher reliability compared to the conventional EF. In addition, since the soft symbols in the CEF-CS protocol are more polarized than those in the EF protocol (as seen from Fig. 3.1), it is more suitable to implement compressive sensing in our CEF-CS.

3.4.2 Received SNR

According to [27], the soft symbol of x_i^q is modeled as $\tilde{x}_i^q = \psi_i (x_i^q + e_i)$, where e_i is the soft noise, and ψ_i represents the scalar factor which makes the soft noise e_i uncorrelated to the information symbol x_i^q. We have $\mathcal{E}(e_i x_i^q) = 0$ and $\psi_i = \frac{\mathcal{E}(x_i^q \tilde{x}_i^q)}{\mathcal{E}((x_i^q)^2)}$. Similarly, the network coded symbol is modeled as $\tilde{x}_{\mathcal{R}}^q = \psi_{EF}(x_1^q x_2^q + e_{EF})$, where e_{EF} is the soft noise, and ψ_{EF} represents the scalar factor which makes e_{EF} uncorrelated to the network coded symbol $x_1^q x_2^q$.

3.4 Performance Analysis and Comparison

In the conventional EF, the relay forwards $\tilde{x}_{\mathcal{R}}^q$ in Eq. (3.9) without compression. At the destination, the receiver first estimates x_i^q from the received signal $y_{i\mathcal{D}}^q$ and obtains $\tilde{x}_i^q = \tanh(LLR_{d,x_i^q}/2)$, where LLR_{d,x_i^q} is the LLR of x_i^q at the destination. Then $\tilde{x}_i^q$ is multiplied with $y_{\mathcal{R}\mathcal{D}}^q$ in order to cancel $x_{\bar{i}}^q$, where $\bar{i} = 1, 2$ and $\bar{i} \neq i$. By defining $\kappa = \sqrt{\frac{E_{\mathcal{R}}}{\mathcal{E}[|\tilde{x}_{\mathcal{R}}|^2]}}$, we have

$$
\begin{aligned}
y_{\mathcal{R}\mathcal{D}}^q \tilde{x}_i^q &= \left(\kappa h_{\mathcal{R}\mathcal{D}} \psi_{EF} \left(x_1^q x_2^q + e_{EF}\right) + n_{\mathcal{R}\mathcal{D}}^q\right)\left(\psi_i \left(x_i^q + e_i\right)\right) \\
&= \kappa h_{\mathcal{R}\mathcal{D}} \psi_{EF} \psi_i x_{\bar{i}}^q + \kappa h_{\mathcal{R}\mathcal{D}} \psi_{EF} \psi_i e_i x_1^q x_2^q + \kappa h_{\mathcal{R}\mathcal{D}} \psi_{EF} \psi_i e x_i^q + \\
&\qquad \kappa h_{\mathcal{R}\mathcal{D}} \psi_{EF} \psi_i e_i e_{EF} + \psi_i n_{\mathcal{R}\mathcal{D}}^q x_i^q + \psi_i e_i n_{\mathcal{R}\mathcal{D}}^q, \quad (3.10)
\end{aligned}
$$

where noise item, denoted by $N_{i,EF} = \kappa h_{\mathcal{R}\mathcal{D}} \psi_{EF} \psi_i \left(e_i x_1^q x_2^q + e x_i^q + e_i e_{EF}\right) + \psi_i \left(n_{\mathcal{R}\mathcal{D}}^q x_i^q + e_i^q n_{\mathcal{R}\mathcal{D}}^q\right)$, can be approximated as Gaussian distributed [27] with mean μ_i and variance σ_i^2. Since $\mathcal{E}\left[e_i x_i^q\right] = 0$, we have $\mu_i = 0$ and $\sigma_i^2 = \kappa^2 h_{\mathcal{R}\mathcal{D}}^2 \psi_{EF}^2 \psi_i^2 \left(\sigma_{e_i}^2 + \sigma_e^2 + \sigma_{e_i}^2 \sigma_e^2\right) + \psi_i^2 \left(\sigma^2 + \sigma_{e_i}^2 \sigma^2\right)$, where $\sigma_{e_{EF}}^2$ and $\sigma_{e_i}^2$ are the variances of e_{EF} and e_i, respectively.

Based on Eq. (3.10), we can obtain the LLR for x_i^q, which is then combined with $y_{i\mathcal{D}}^q$ to make the decision on $x_{\bar{i}}^q$. Here, we investigate the received SNR in Eq. (3.10), which can be expressed as

$$
\rho_{i,EF} = \frac{\kappa^2 h_{\mathcal{R}\mathcal{D}}^2 \psi_{EF}^2 \psi_i^2}{\kappa^2 h_{\mathcal{R}\mathcal{D}}^2 \psi_{EF}^2 \psi_i^2 \left(\sigma_{e_i}^2 + \sigma_{e_{EF}}^2 + \sigma_{e_i}^2 \sigma_{e_{EF}}^2\right) + \psi_i^2 \left(\sigma^2 + \sigma_{e_i}^2 \sigma^2\right)}. \quad (3.11)
$$

For the CEF-CS, the network coded soft symbol vector $\tilde{x}_{\mathcal{R}}$ are compressed at the relay. When recovering $\tilde{x}_{\mathcal{R}}$ at the destination with BP, errors could be introduced [58], i.e., $\hat{\tilde{x}}_{\mathcal{R}} = \tilde{x}_{\mathcal{R}} + n_{qu}$, where n_{qu} is the quantization noise. Denote $\hat{\tilde{x}}_{\mathcal{R}}^q$ and $\hat{n}_q^q$ the q-th symbols in $\hat{\tilde{x}}_{\mathcal{R}}$ and n_{qu}, respectively. The recovered symbol $\hat{\tilde{x}}_{\mathcal{R}}^q$ is multiplied with $\tilde{x}_i^q$ in order to cancel $x_{\bar{i}}^q$. Then we have

$$
\begin{aligned}
\hat{\tilde{x}}_{\mathcal{R}}^q \tilde{x}_i^q &= \left(\psi_{CEF-CS} \left(x_1^q x_2^q + e_{CEF-CS}\right) + n_{qu}^q\right)\left(\psi_i \left(x_i^q + e_i\right)\right) \\
&= \psi_{CEF-CS} \psi_i x_{\bar{i}}^q + \psi_{CEF-CS} \psi_i e_i x_1^q x_2^q + \psi_{CEF-CS} \psi_i e_{CEF-CS} x_i^q \\
&\qquad + \psi \psi_i e_i e_{CEF-CS} + \psi_i n_{qu}^q x_i^q + \psi_i e_i n_{qu}^q, \quad (3.12)
\end{aligned}
$$

where the noise item, denoted by
$N_{i,CEF-CS} = \psi_{CEF-CS} \psi_i \left(e_i x_1^q x_2^q + e_{CEF-CS} x_i^q + e_i e_{CEF-CS}\right) + \psi_i \left(x_i^q n_{qu}^q + e_i n_{qu}^q\right)$, can

be approximated as Gaussian distributed with mean μ_i and variance σ_i^2. Since $\mathcal{E}\left[e_i x_i^q\right] = 0$ and n_{qu}^q is independent from the signal, we have $\mu_i = 0$ and $\sigma_i^2 = \psi^2 \psi_i^2 \left(\sigma_{e_i}^2 + \sigma_e^2 + \sigma_{e_i}^2 \sigma_e^2\right) + \psi_i^2 \left(\sigma_q^2 + \sigma_{e_i}^2 \sigma_q^2\right)$, where σ_q^2 is the variance of n_{qu}. The received SNR in Eq. (3.12) can be written as

$$\rho_{i,CEF-CS} = \frac{\psi_{CEF-CS}^2 \psi_i^2}{\psi_{CEF-CS}^2 \psi_i^2 \left(\sigma_{e_i}^2 + \sigma_{e_{CEF-CS}}^2 + \sigma_{e_i}^2 \sigma_{e_{CEF-CS}}^2\right) + \psi_i^2 \left(\sigma_q^2 + \sigma_{e_i}^2 \sigma_q^2\right)}. \quad (3.13)$$

3.5   Simulation Results

In the simulations, we consider quasi-static Rayleigh fading channels, and assume that each source transmits $l = 200$ BPSK symbols in a transmission period and run 1000 block errors to obtain simulation results. Also, we assume that the distances $d_{S_i R}$ and d_{RD} are equal to 0.5, and $d_{S_i D}$ is equal to 1. The attenuation exponent γ is set to be 2, and the sources and the relay have unit transmission power, namely, $E_\mathcal{S} = E_\mathcal{R} = 1$. When applying the CS at the relay in the CEF-CS and EF-CS protocols, we denote by r the transmission rate at the relay, which means that the encoding matrix is of size $lr \times l$, and correspondingly the number of measurements transmitted from relay is $m = lr$.

Firstly, we investigate the BER performance of the CEF-CS protocol under different source correlation coefficients shown in Fig. 3.3. The system BER is defined as the average value of BERs of the two sources' signal at the destination. Note that the correlation coefficient of the two sources is defined in Eq. (3.3), which is derived from τ. Therefore, in Fig. 3.3, we simulate the system BERs for different values of τ. Also, in Fig. 3.3, we consider the SNRs of 10dB, 15dB and 20dB and a transmission rate $r = 1/2$. As can be seen from Fig. 3.3, with the increase of the value of τ, the BER performance becomes worse. This is because that increased τ, i.e., the reduced source correlation, leads to the less sparsity of the network coded soft symbol vector. Furthermore, we can see from Fig. 3.3 that when τ exceeds 0.5, the system can only achieve a diversity gain of 1; when τ falls below 0.3, the diversity gain is close to 2.

Secondly, we study the impact of the transmission rate r on the BER performance for the CEF-CS protocol for a fixed τ. Here, we choose $\tau = 0.2$ since it offers a good error performance as shown in Fig. 3.3. We investigate the system BERs with different transmission
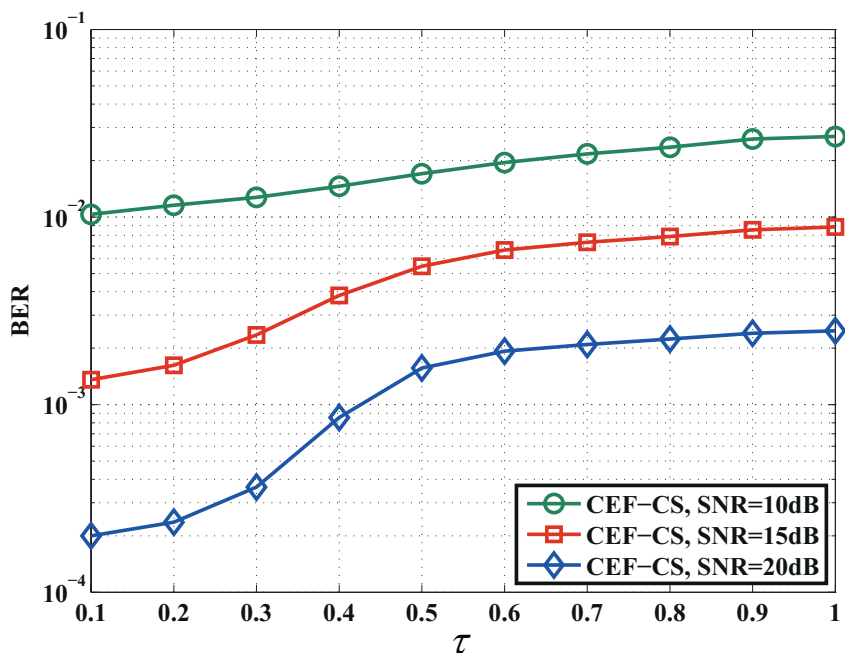
Figure 3.3: BER performance of the CEF-CS protocol under different source correlation models, at $SNR = 10dB$, $SNR = 15dB$ and $SNR = 20dB$, and with $r = 1/2$.

rates r under the SNRs of 10dB, 15dB and 20dB. As can be seen from Fig. 3.8, with the increase of r, the BER performance will gradually become better. Also, when r exceeds 0.5, the system diversity gain becomes closer to 2.

Thirdly, we investigate the received SNRs discussed in Section 3.4.2. We compare our CEF-CS protocol with two other protocols, namely, the conventional EF protocol, the CEF protocol, with $\tau = 0.2$. Specifically, in the CEF, the relay directly forwards the network coded soft symbol vector calculated by Eq. (3.4) without any compression. The received SNRs in Fig. 3.5 for the EF and the CEF-CS protocols are calculated from Eq. (3.11) and Eq. (3.13), respectively. The received SNR for the CEF protocol can be obtained by following the similar method as in the EF protocol. We can see from Fig. 3.5 that the received SNR of the CEF protocol always outperforms that of the EF protocol. However, the gap between the received SNRs of the CEF and EF goes to zero in the high SNR region, which means that the error performance of these two protocols tend to be equal in the high SNR region. For the CEF-CS protocol, it is shown that the CEF-CS with $r = 2/10$ obtains lower receiver SNR than that in the EF and CEF protocols. For the transmission rate $r = 7/10$, the CEF-CS has the best receiver SNR compared to the other protocols. This is due to the fact that the quantization
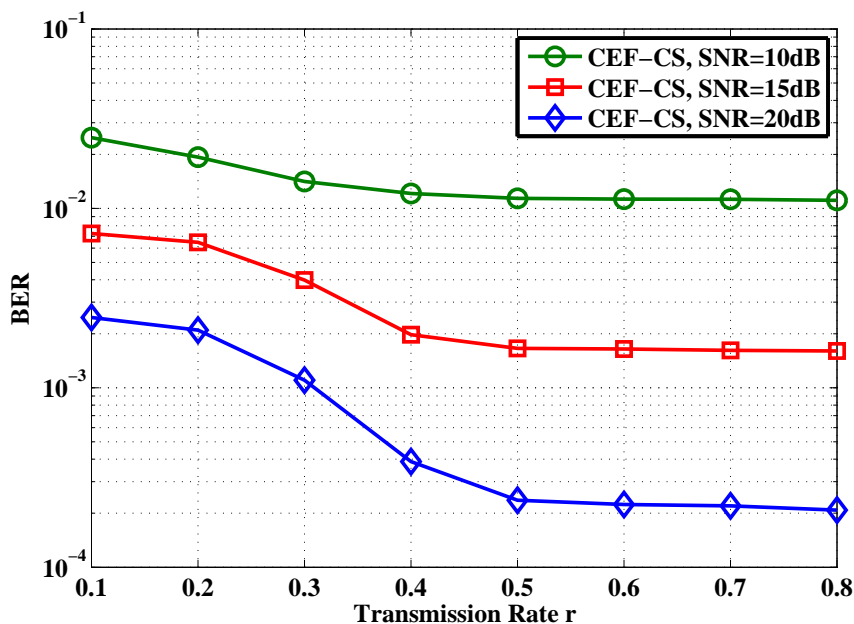
Figure 3.4: BER as a function of the transmission rate r in the CEF-CS protocol, at $SNR = 10dB$, $SNR = 15dB$ and $SNR = 20dB$, and with $\tau = 0.2$.

noise n_{qu}^q in Eq. (3.12) is strictly constrained in the range of $(0, 2)$, while the value range of $n_{\mathcal{RD}}$ in Eq. (3.10) is infinite. In particular, when SNR is large enough, the majority of n_{qu}^q gathers around 0. We compare the PDF of quantization noise with that of $(n_{\mathcal{RD}}/(\kappa h_{\mathcal{RD}}))$ when the CS transmission rate r is $1/2$ in Fig. 3.6 and clearly see that the overall quantization noise item has relatively smaller value than $(n_{\mathcal{RD}}/(\kappa h_{\mathcal{RD}}))$, which leads to the higher receiver SNR of the CEF-CS protocol than the EF protocol.

Fourthly, we investigate the BER performance of the CEF-CS, the CEF, and the EF protocols. We also consider another benchmark protocol, namely, the EF-CS, where the relay applies CS to the network coded soft symbol vector obtained from the EF protocol. As can be seen from Fig. 3.7, when $\tau = 0.2$, the CEF-CS protocol with rate $2/10$, and the EF-CS protocol with rate $2/10, 7/10$ can only achieve a diversity gain of one, while the CEF-CS with rate $7/10$, the CEF, and the EF can achieve a diversity gain of two. The worse performance of the EF-CS implies that the CS is not suitable for the EF. This is because that the soft symbol vector in the EF does not ensure the sparsity for CS. Besides, the CEF outperforms the CEF-CS with rate $7/10$, and the CEF-CS with rate $7/10$ outperforms the EF. However, the performance gap between these three protocols goes to zero in the high SNR region. We also compare the BER performance of the CEF-CS protocol under other correlation models,
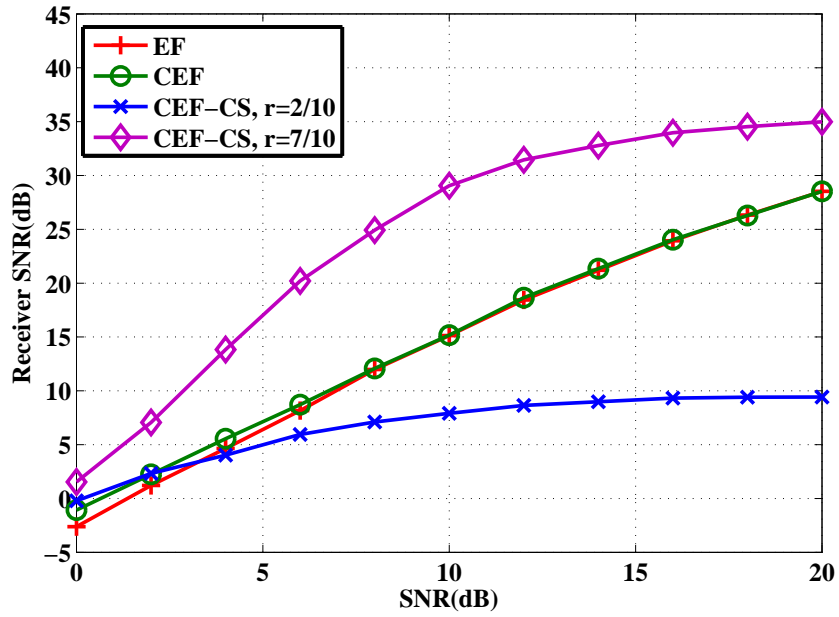
Figure 3.5: Receiver SNR vs transmission SNR, when $\tau = 0.2$.
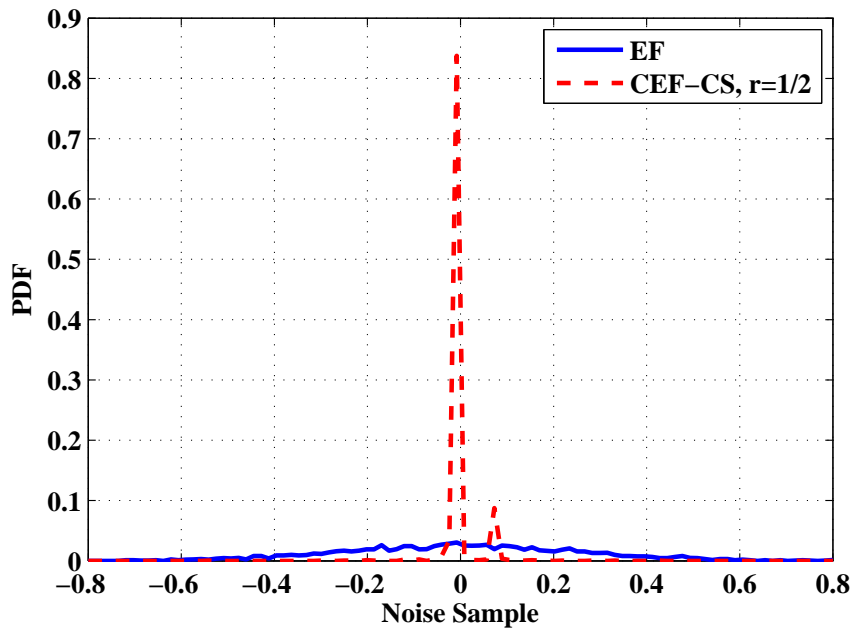

Figure 3.6: The comparison between the noise samples of $(\hat{\tilde{x}}_{\mathcal{R}} - \tilde{x}_{\mathcal{R}})$ and $(n_{\mathcal{RD}}/(\kappa h_{\mathcal{RD}}))$, when $\tau = 0.2$, $r = 1/2$ and $SNR = 5dB$.
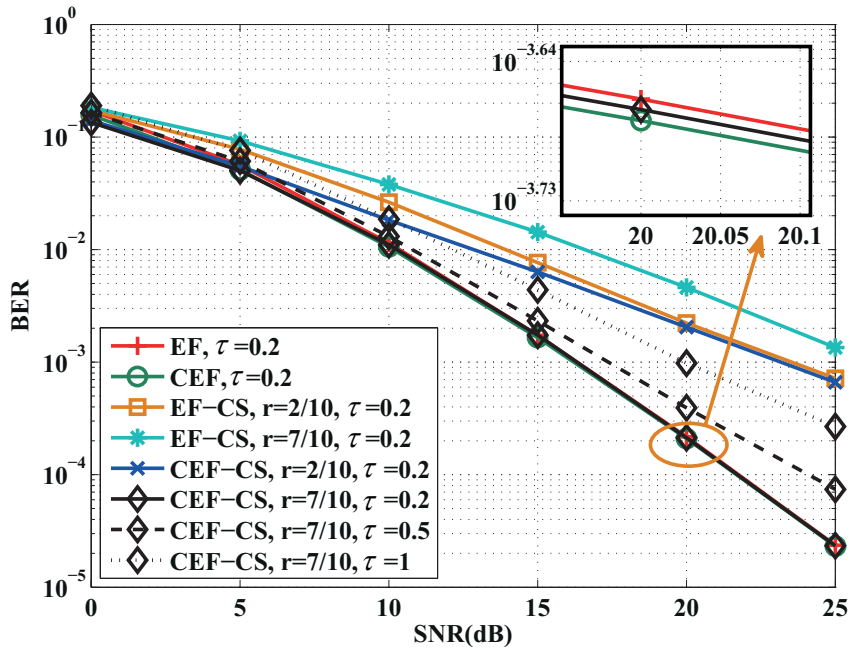
Figure 3.7: BER performance of different schemes over fading channels.

namely $\tau = 0.5$ and $\tau = 1$. As can be seen, with the decrease of the correlation, the BER performance becomes worse. We also investigate the impact of the transmission rate r on the BER performance for the CEF-CS and the EF-CS protocols in Fig. 3.8, where SNR is set to be 15dB and 20dB, and $\tau = 0.2$. Fig. 3.8 further verifies the infeasibility to apply CS directly on the conventional EF protocol. It shows that with the increase of the transmission rate, the performance of the EF-CS protocol becomes worse. This is because the CS does not promise recovery for the soft symbols generated from the EF protocol, while the power allocated on each symbol is reduced with a higher transmission rate.

Furthermore, since the relay node uses less time slots to forward information in the compressed protocols, the throughput performance of the compressed protocols will be much improved. Specifically, we define the throughput Tr as the number of the correctly received symbols out of the number of the entire transmitted symbols per transmission period, which can be calculated by

$$Tr = \frac{2l - e}{2l + m},\tag{3.14}$$

where e denotes the number of symbol errors for both sources, l is the length of the source signal, and m is the length of the signal transmitted from the relay node. For the EF and
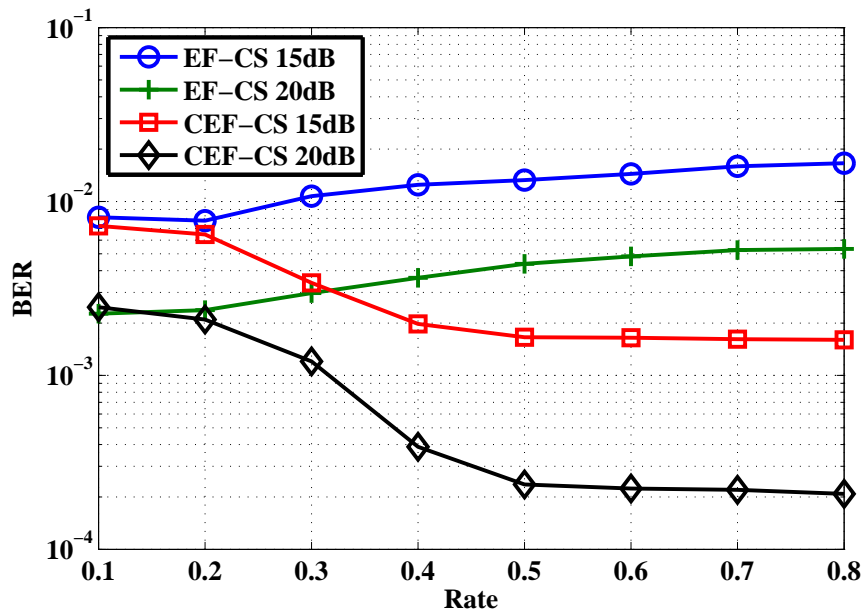
Figure 3.8: BER as a function of the transmission rate r in the CEF-CS and EF-CS protocols, at $SNR = 15dB$ and $SNR = 20dB$ when $\tau = 0.2$.

CEF protocols without CS, m is constantly equal to l. For the CEF-CS protocol, we have $m < l$ due to CS. As is shown in Fig. 3.7, the EF, the CEF and the CEF-CS at $r = 7/10$ have equivalent BER performance. However, in terms of the throughput performance, the CEF-CS at $r = 7/10$ will improve 10% compared with the EF and the CEF protocols, as shown in Fig. 3.9.
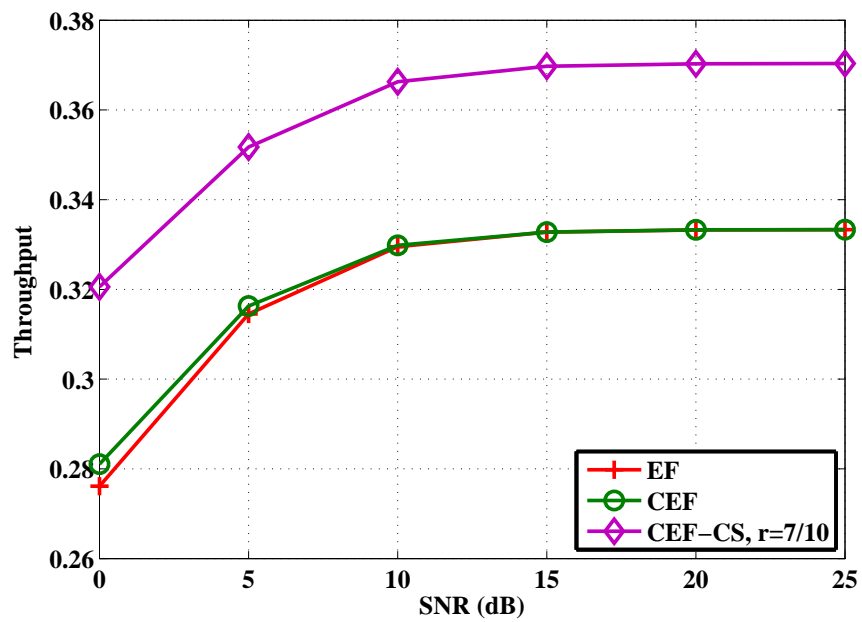
Figure 3.9: BER performance of different schemes over fading channels.

Chapter 4

A Soft Information Delivery Scheme in Two-Way Relay Channels with Network Coding

In this chapter, we propose a practical 1-bit soft forwarding protocol for a network coded TWRC. Different from the conventional EF protocol, the proposed protocol forwards 1-bit soft information at the relay. We employ the joint TCQ/M to implement 1-bit transmission of the soft information. Also, the codebooks in the TCQ are designed to be adaptive to the source-to-relay channel conditions so that the system can achieve the full diversity gain over fading channels. Specifically, in the low source-to-relay channel SNR region, we apply the TCQ/M to the soft information based on the codebook generated by the Lloyd-Max quantizer. In the high source-to-relay channel SNR region, where the soft information is equivalent to its hard decision, we design the codebook by repeating the soft information. It has been shown that the proposed protocol outperforms both the AF and the DF protocols over fading channels.

4.1   Introduction

The recent emerging relay strategies have been shown significant advantages for most future wireless applications. Two of these relay strategies are the AF protocol [75] and the DF protocol [25], which have been widely studied in the literature. To overcome the disadvantages of the AF and the DF protocols explained in Section 2, SIF protocols [82] have been raised. One of the SIF based protocol is called EF [77]. It has been shown in [77] that the EF protocol outperforms the AF and DF protocols in the one-way relay channels. Recently, TWRC have become increasingly appealing to both academia and industry. That is mainly because network coding can be employed to achieve higher spectral efficiency. Quite a few relay strategies have been proposed in the TWRC, e.g., [28, 38].

In particular, the soft network coding protocol proposed for the TWRC in [38] has attracted a lot of attention. However, it was assumed in [38] that the relay-to-source channels have limitless bandwidth. Therefore, the soft information can be transmitted to each source from the relay without quantization. In practice, due to the finite channel bandwidth, we need to quantize the soft information before transmission. However, even if we quantize the soft information into a limited number of bits, it still has a much lower spectrum efficiency than the DF protocol. Therefore, 1-bit soft forwarding is an attractive approach to achieving better performance than the DF with the same bandwidth. The TCQ/M scheme is one of the quantization schemes that can realize 1-bit quantization with a good error performance [68, 73, 74, 83], because the quantization noise can be reduced without rate increase if a structured codebook with an expanded set of quantization levels is used. Although any modulation scheme can be used in conjunction with the TCQ, it is shown that a joint TCQ/M system ensures that the squared distance between the channel sequences is commensurate with the squared error in the quantization [73, 74].

In this work, we are interested in designing a practical 1-bit soft forwarding protocol based on the joint TCQ/M in the TWRC over fading. Also, we design adaptive codebooks in the TCQ based on different source-to-relay channel conditions. This is because the probability distribution of the soft information varies with different SNR values of the source-to-relay channels. Specifically, the PDF of the soft information presents approximately a Gaussian distribution in the low channel SNR region. On the other hand, the values of the soft information are equivalent to hard decisions in the high channel SNR region. This work applies the

TCQ/M to the soft information by using codebooks generated from the Lloyd-Max quantizer in the low channel SNR region, which we define as the EF with TCQ scheme throughout the chapter. In the high channel SNR region, where the soft information is equivalent to its hard decision, the codebook is designed by repeating the soft information, and the scheme is defined as the EF with TCQ codewords repeat scheme. It is shown in the simulation that the proposed protocol outperforms both the AF and the DF protocols over the fading channels. It also closely approximates the performance of the conventional EF protocol where the soft information is assumed to be transmitted without quantization.

4.2   System Model

As shown in Fig. 2.1, in the TWRC, the two sources transmit or receive information at different time slots. At the first time slot, $\mathcal{S}_1$ transmits its own signals to both the relay and $\mathcal{S}_2$. At the second time slot, $\mathcal{S}_2$ transmits its own signals to both the relay and $\mathcal{S}_1$. The received signal at the relay from each source and the received signal from the direct link can be respectively calculated by

$$\boldsymbol{y}_{i\mathcal{R}} = h_{i\mathcal{R}}\sqrt{E_i}\boldsymbol{x}_i + \boldsymbol{n}_{i\mathcal{R}},$$

$$\boldsymbol{y}_{ij} = h_{ij}\sqrt{E_i}\boldsymbol{x}_i + \boldsymbol{n}_{ij}, \tag{4.1}$$

where $\boldsymbol{x}_i = (x_i^1, \cdots, x_i^l)^T$, $x_i^q \in \{\pm 1\}$ and $q \in \{1, \cdots, l\}$, represents signals transmitted from either of the two sources $\mathcal{S}_i$, BPSK modulated. E_i is defined as the transmission power at both sources, h_{ij} and $h_{i\mathcal{R}}$ represent the channel coefficient between two sources, and the channel coefficient between each source S_i and the relay, respectively. Vectors $\boldsymbol{n}_{ij} = (n_{ij}^1, \cdots, n_{ij}^l)^T$ and $\boldsymbol{n}_{i\mathcal{R}} = (n_{i\mathcal{R}}^1, \cdots, n_{i\mathcal{R}}^l)^T$ are the noise sample at the source and the relay, which are both defined as Gaussian distributed with zero mean value and variance σ^2. Vectors $\boldsymbol{y}_{i\mathcal{R}} = (y_{i\mathcal{R}}^1, \cdots, y_{i\mathcal{R}}^l)^T$ and $\boldsymbol{y}_{ij} = (y_{ij}^1, \cdots, y_{if}^l)^T$ represent the signal received at the relay and the other source from one source, respectively. As for the SNR of the source-to-relay channel, it can be defined by $\rho_{i\mathcal{R}} \triangleq h_{i\mathcal{R}}^2 E_i / \sigma^2$.

At the third time slot, the relay processes the received signals and then broadcasts the processed signal to both $\mathcal{S}_1$ and $\mathcal{S}_2$. In this stage, we apply the TCQ to the soft network coded
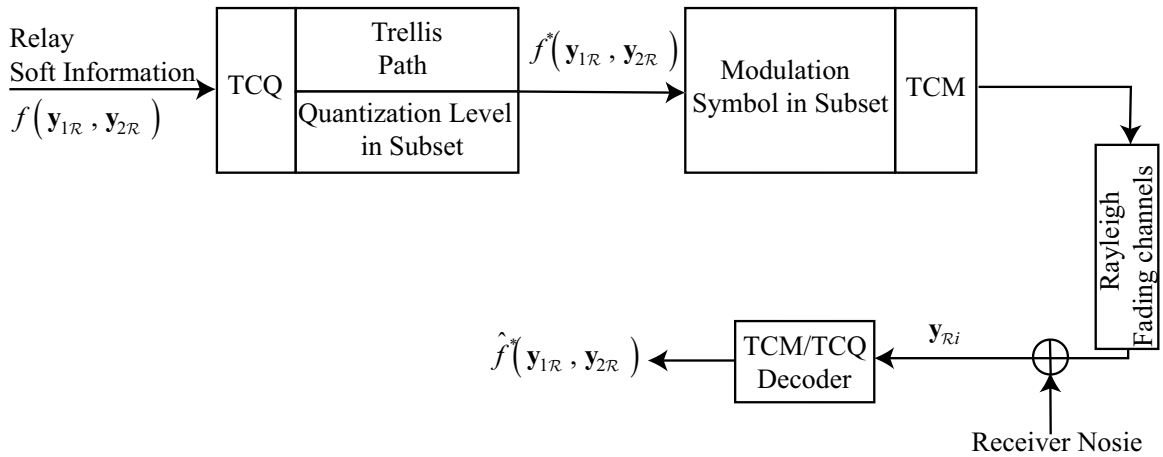
Figure 4.1: Joint TCQ/M system in relay networks.

symbols defined in [38]. We first form the network coded symbols from the conventional EF protocol. Then we use the TCQ to implement the quantization over the power-normalized relay function calculated in Eq. (2.6). For simplicity, we eliminate the subscript of the EF in Eq. (2.6), denoting by $f(\boldsymbol{y}_{1\mathcal{R}}, \boldsymbol{y}_{2\mathcal{R}})$ the relay function vector of the EF protocol, and denote $f^*(\boldsymbol{y}_{1\mathcal{R}}^q, \boldsymbol{y}_{2\mathcal{R}}^q)$ as the quantized relay function vector, and both vectors are of length l. A joint TCQ/M system follows after the power-normalized relay function is calculated, as shown in Fig. 4.1. For the TCQ/M at rate 1, quadrature phase-shift keying (QPSK) is employed as the modulation technique. Then the signal received by each source from the relay can be given by

$$\boldsymbol{y}_{\mathcal{R}i} = \sqrt{E_\mathcal{R}} h_{\mathcal{R}i} f^*(\boldsymbol{y}_{1\mathcal{R}}, \boldsymbol{y}_{2\mathcal{R}}) + \boldsymbol{n}_{\mathcal{R}i}, \tag{4.2}$$

where $h_{\mathcal{R}i}$ represents the channel coefficient between the relay and the source, which is modeled as an independent zero mean Gaussian random variable with unit variance. $\boldsymbol{n}_{\mathcal{R}i}$ is the noise sample vector at each source, which consists of the complex additive white Gaussian noise (AWGN) samples with per-dimension mean value zero and variance $\sigma^2/2$. As shown in Fig. 4.1, the received quantized signal at the output of the TCQ/M decoder is denoted by

$$\hat{f}^*(\boldsymbol{y}_{1\mathcal{R}}, \boldsymbol{y}_{2\mathcal{R}}) = f(\boldsymbol{y}_{1\mathcal{R}}, \boldsymbol{y}_{2\mathcal{R}}) + \boldsymbol{n}_{equiv\_\mathcal{R}i}, \tag{4.3}$$

where $\hat{f}^*(\boldsymbol{y}_{1\mathcal{R}}, \boldsymbol{y}_{2\mathcal{R}})$ denotes the received quantized signal vector, and $\boldsymbol{n}_{equiv\_\mathcal{R}i}$ is regarded as the quantization noise vector. According to Eq. (2.25), the variance of $\boldsymbol{n}_{equiv\_\mathcal{R}i}$ in Eq. (4.3) can be expressed as $\rho_m\left(f\left(\boldsymbol{y}_{1\mathcal{R}}, \boldsymbol{y}_{2\mathcal{R}}\right), \hat{f}^*\left(\boldsymbol{y}_{1\mathcal{R}}, \boldsymbol{y}_{2\mathcal{R}}\right)\right)$.

At the receiver, the decoding is accomplished by first using the Viterbi algorithm to find

the path which has the MMSE to the received signals, and then mapping the selected path back into the TCQ levels. The received quantized signal $\hat{f}^*(\boldsymbol{y}_{1\mathcal{R}}, \boldsymbol{y}_{2\mathcal{R}})$ at $\mathcal{S}_i$ from the relay is multiplied with $\boldsymbol{x}_i$ to cancel the source's own signal, which is then combined with $\boldsymbol{y}_{ji}$ to make a hard decision on each symbol in the vector $\boldsymbol{x}_j$.

4.3 Soft Information Quantization

In order to compete with the DF protocol whose transmission rate is 1 at the relay, we utilize the TCQ at rate 1 to implement the quantization. We assume that channels between all terminals experience independent quasi-static Rayleigh fading. In other words, channel coefficients keep constant during an *m*-symbol block but change independently to the next block. Due to the slow fading, it is possible for receivers to accurately estimate the channel-state-information (CSI) at all receivers. Besides, the codebook for the TCQ should be synchronized at both the relay and receivers. This can be achieved by presetting different codebooks for the TCQ according to different source-to-relay channel SNRs. The source-to-relay CSI is known to the relay, and the destination also knows the source-to-relay CSI; thus, the synchronization can be achieved.

4.3.1 The PDF of the Soft Symbol

In this work, we employ the Lloyd-Max quantizer [71, 72] to determine the codebook for each block in the TCQ when the source-to-relay channel SNR is low. Similar systems can be established based on other quantization methods, such as the equiprobable output quantizer [84]. The Lloyd-Max quantizer can be an insight for other methods. For a quantizer with Q reproduction levels, the Lloyd algorithm is applied to minimize the mean squared error distortion, which is given by

$$D_Q = \mathcal{E}\left\{(f(\boldsymbol{y}_{1\mathcal{R}}, \boldsymbol{y}_{2\mathcal{R}}) - f^*(\boldsymbol{y}_{1\mathcal{R}}, \boldsymbol{y}_{2\mathcal{R}}))^2\right\} = \sum_{i=1}^{Q} \int_{b_i}^{b_{i+1}} (l - c_i)^2 p(l) dl, \qquad (4.4)$$

where b_i denotes the decision boundary, c_i represents the ith reproduction level, and $p(l)$ is the PDF of the signal that shall be quantized. The optimization can be solved iteratively by employing the Lloyd algorithm. In each iteration, the optimized decision boundary lies in the middle of two successive reproduction levels, i.e. $b_i = \frac{c_{i-1}+c_i}{2}$; the reproduction level is optimized by the centroid of the decision intervals, i.e. $c_i = \frac{\int_{b_i}^{b_{i+1}} lp(l)dl}{\int_{b_i}^{b_{i+1}} p(l)dl}$. For each network coded soft symbol $\mathcal{E}\left(x_1^q x_2^q | y_{1\mathcal{R}}^q, y_{2\mathcal{R}}^q\right)$ defined in Eq. (2.4), its PDF is given by

$$p_{\mathcal{E}\left(x_1^q x_2^q | y_{1\mathcal{R}}^q, y_{2\mathcal{R}}^q\right)}(z) = \int \frac{1}{|y|} p_{\mathcal{E}\left(x_2^q | y_{2\mathcal{R}}^q\right)}(y) \, p_{\mathcal{E}\left(x_1^q | y_{1\mathcal{R}}^q\right)}\left(\frac{z}{y}\right) dy, \tag{4.5}$$

in which, the PDF of $\mathcal{E}\left(x_i^q | y_{i\mathcal{R}}^q\right)$ can be expressed as

$$p_{\mathcal{E}\left(x_i^q | y_{i\mathcal{R}}^q\right)}(t) = \frac{1}{2}\left[p_{\mathcal{E}\left(x_i^q | y_{i\mathcal{R}}^q\right)|x_i^q}(t|x=1) + p_{\mathcal{E}\left(x_i^q | y_{i\mathcal{R}}^q\right)|x_i^q}(t|x=-1) \right]. \tag{4.6}$$

As the BPSK modulation is applied in the source-to-relay channel and the additive Gaussian white noise (AWGN) is considered at the relay, the conditional PDF of $\mathcal{E}\left(x_i^q | y_{i\mathcal{R}}^q\right)$ based on x_i^q in Eq. (4.6) is calculated as

$$p_{\mathcal{E}\left(x_i^q | y_{i\mathcal{R}}^q\right)|x_i^q}(t|x) = \frac{\sigma^2}{h_{i\mathcal{R}}(1-t^2)} \frac{1}{\sqrt{2\pi}\sigma} \exp\left\{ -\frac{1}{2\sigma^2}\left[\frac{\sigma^2}{2h_{i\mathcal{R}}} \ln\left(\frac{1+t}{1-t}\right) - h_{i\mathcal{R}}x \right]^2 \right\}. \tag{4.7}$$

According to Eq. (4.5), Eq. (4.6) and Eq. (4.7), the reproduction levels are evaluated by numerical integration in the simulation. When the source-to-relay channel SNR is high, however, the use of the codebook generated by the Lloyd algorithm may lead to erroneous mapping in the trellis diagram. The reason is explained as follows. Based on the analysis of Eq. (2.6), there may still exist very few small numbers in large blocks, even though the network symbols in the relay function $f(\boldsymbol{y}_{1\mathcal{R}}, \boldsymbol{y}_{2\mathcal{R}})$ approach 1 or -1. This is due to the occasional big noise at the receiver and random fading channel. By employing the Lloyd algorithm, such small numbers will appear in the codebook. As long as the structure of the convolutional encoder is set—the branch labeling in the trellis is set—such codebooks and the mapping principle given in Eq. (2.24) may map 1 or -1 into the small numbers, which decreases the reliability of the real values.

4.3.2   Repeating Codewords

As the bad performance of the TCQ results from the unreasonable selection of the codebook when the source-to-relay channel SNR is high, we may refine the codebook in order to prevent mapping errors from occurring under the high channel SNR region. Motivated by Eq. (2.24), instead of selecting the path which minimizes the MSE between the two m-symbol sequences, we decide to minimize the MSE between each symbol and the corresponding reproduction level. This process can be treated as minimizing the following equation

$$d(\boldsymbol{x}, \hat{\boldsymbol{x}}) = \sum_{i=1}^{m} d_i(x_i, \hat{x}_i),$$

where

$$d_i(x_i, \hat{x}_i) = \sqrt{(x_i - \hat{x}_i)^2} = |x_i - \hat{x}_i|. \tag{4.8}$$

Alternatively, Eq. (4.8) requires that for each state in the trellis, the branches entering or leaving the state should represent all possible codewords. And this can be simply achieved by repeating codewords in the codebook. The explanation is given by a rate-$1/2$ convolutional encoder shown in the left side of Fig. 2.6. The corresponding branch labeling is shown in the right side with reproduction levels c_i, $i = \{1, 2, 3, 4\}$. With such an encoder, for an integral encoding rate 1, the size of the codebook is $2^{1+1} = 4$. To guarantee correct mapping under the high source-to-relay channel SNR region where the soft information is equivalent to hard decision, codewords need to be repeated. Hence in the codebook of length four, only two different codewords can exist, namely 1 and -1. Then, the codebook consists of four codewords, i.e. -1, -1, 1, and 1. There are several ways to sort the four codewords in a codebook which can guarantee the accurate quantization, provided that TCM symbols mapping is consistent with the order of the codebook. For instance, if the QPSK with natural mapping shown in Fig. 4.2 is used as the modulation technique, and the branch labeling is depicted on the right side of Fig. 2.6, one possible codebook can be [-1 1 1 -1] corresponding to the modulation symbols [00 01 10 11]. As can be seen from Fig. 4.2, when -1 is mapped to both 00 and 11 symbols, and 1 is mapped to both 01 and 10 symbols, the overall QPSK constellation can be regarded as the BPSK constellation which expands the distance between different codewords.

We refer to the scheme where repeated codebook is utilized as the codewords repeat scheme.
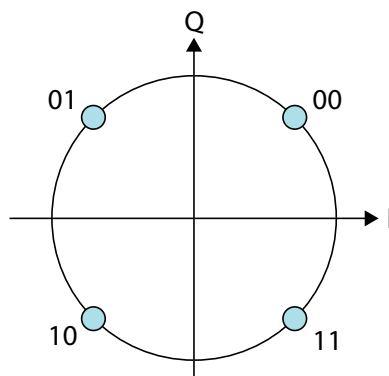
Figure 4.2: Constellation diagram for QPSK with natural mapping.

To better demonstrate the mechanism of the codewords repeat scheme, we give an example as follows. We regard a chain of 10 numbers as a miniature of the hundreds of transmitted samples from the relay, and give an example that the chain is $(-1, -1, 1, -1, -1, 0.19, 1, 1, -0.4, -1)$. With a rate-$1/2$ convolutional encoder, for integral rate R b/sample encoding, 2^{R+1} reproduction levels (codewords) are used, and with Lloyd-Max quantizer, we can get the output alphabet for TCQ from the set of output points of Lloyd-Max quantizer. In reality, the codebook for each incoming sequence can be obtained easily. For different channel SNR, a very long train of soft information at the relay can be generated, and a statistically featured codebook can be found via the quantizer. Under this very circumstance, the output codebook is $\mathcal{C} = (-1, -0.4, 0.19, 1)$. Then the codewords are mapped into 4 subsets, each of 2^{R-1} codewords. As it can be easily seen, with the codebook $(-1, -0.4, 0.19, 1)$, each sample in the chain can find the same value as itself in the four codewords. However, with a conventional TCQ, we still use a rate-$1/2$ convolutional encoder shown in Fig. 2.6, when mapping each sample on the trellis, we have the output $(-1, -0.4, 0.19, -1, -1, 0.19, 1, 1, 0.19, -1)$, which is quite different from the input. It is shown in the Fig. 4.3 how conventional TCQ leads to a different output although each sample of the input has a same corresponding value in the codebook.

As is mentioned in Eq. (2.24), TCQ uses Viterbi algorithm to select the sequence path representing codewords closest in Euclidean distance to the input. However, it is the selected path which has the shortest Euclidean distance from the input within the defined trellis that encodes the input a wrong sequence. Then we consider adding some branches in the trellis and making the branches added represent the same value as the branch existed, thus making it possible to find the shortest Euclidean distance for each mapping, which means that for
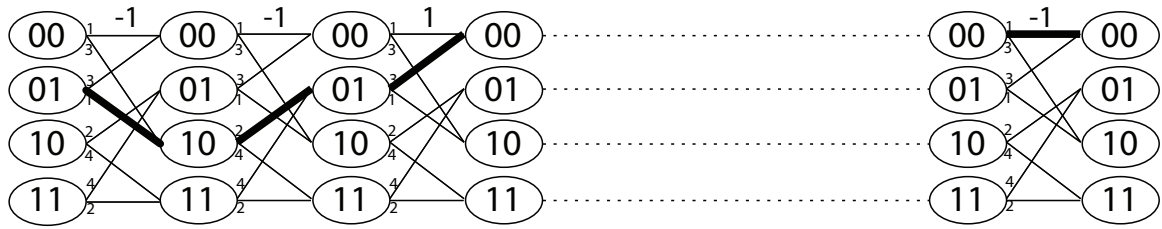
Figure 4.3: Viterbi encoding of the source sequence for 1 bit/sample, and $(5, 2)$ convolutional encoder shown in Fig. 2.6, 4-state trellis.
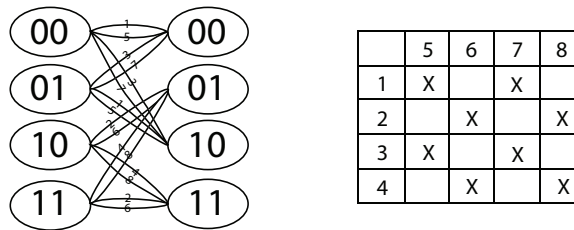
Figure 4.4: 4-state trellis 2 bits/sample and branch added selection.

each incoming sample, let the branch added endue it with the shortest Euclidean distance between one of the quantizer outputs and itself. The process can be treated as minimizing the equation of Eq. (4.8), hence with the increase of number of branches in each trellis, the overall rate of TCQ increases.

4.3.2.1 $R = 2$ **senario**

With the Lloyd-Max quantizer, there are 4 quantization levels corresponding to rate-1 transmission. Then to demonstrate the principle of codewords repeat, duplicating 4 quantization levels leads to 8 quantization levels, which requires rate-2 transmission. To implement the codewords repeat scheme over the trellis, the difference from a conventional TCQ is the branch labels in the trellis might represent the same quantization level. We continue the former example, and still use a rate-$1/2$ convolutional encoder shown in Fig. 2.6 and 4 state trellis to demonstrate how this 2 b/sample TCQ works here.

As can be seen from Fig. 4.4, according to the branch labeling on the left, a table on the right can be used to looked up in order to find the possible codewords repeat for the branches added. The numbers in the right table denote the branch numbers in the trellis. The cross in the table indicates that the current mapping exists. There are $2 \times 2 = 4$ kinds of mapping,

Figure 4.5: 4-state trellis 2 bits/sample and branch added selection.

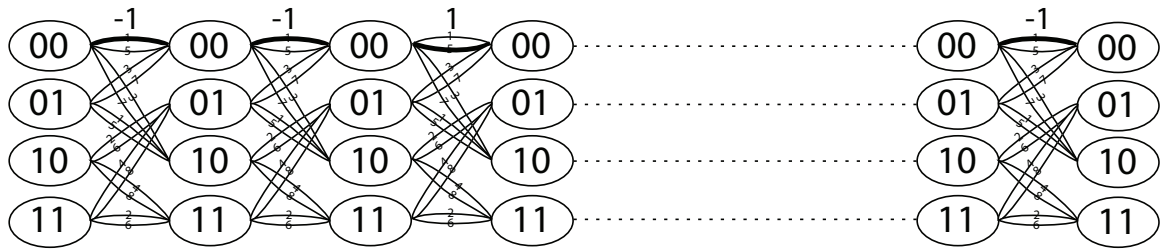namely $(1 = 6, 2 = 5, 3 = 8, 4 = 7), (1 = 6, 2 = 7, 3 = 8, 4 = 5), (1 = 8, 2 = 5, 3 = 6, 4 = 7),$ $(1 = 8, 2 = 7, 3 = 6, 4 = 5)$, and we name it the repeat rule afterwards. It is simple to implement this by repeating old codewords of the Lloyd-Max quantizer.

As for the all 4 kinds of mapping, an exact same chain as the original chain of the ten numbers can be achieved from trellis coded quantization. Fig. 4.5 shows how the trellis diagram obtains the correct mapping. In reality, modulation should be followed after quantization. Then the different kinds of mapping we mentioned above might have different system performance based on different kinds of modulation schemes. Here if conventional joint trellis coded quantization/modulation is used, then for a 2 b/sample TCQ, after quantization, each branch is directly mapped into an 8PSK symbol, which of course, determines that for TCQ/TCM with different repeat rule, the overall performance of TCQ/TCM is different. However, if 2 matched branches are mapped back into the same modulation symbol according to the repeat rule, QPSK can be used although it is 2 b/sample TCQ/TCM. Besides, with QPSK utilized here, the destination node needs to repeat its TCM symbol codewords in accordance with the repeat rule when applying Viterbi algorithm to decode the signal. Therefore, whatever the repeat rule is, the overall performance of TCQ/TCM will not change. Simulation results are showed in the next section.

4.3.2.2 $R = 1$ **scenario**

However, the EF protocol in TWRC utilizes network coding only to save one time slot, and correspondingly in TWRC, the DF protocol with network coding enables the system to decrease one bit transmission from the relay, hence using 2 b/sample to transmit the soft information makes no much sense to comply with using network coding, our ultimate goal is still to implement the quantization with rate 1 b/sample. Take a look at the scenario when

$R = 2$, with the reproduction level repeating, in the codebook of length 8, we only obtain 4 distinguishing reproduction levels. Compared with the scenario when $R = 1$ with no codewords repeating, the BER performance is quite similar under low channel SNR, which will be shown in the simulation section. But with the increase of channel SNR, the scenario $R = 1$ with no codewords repeating shows bad results. Then we designate a threshold for certain feature of the soft information at the relay in the next section.

4.4   Performance Analysis

We first study the threshold for the selection of the codebooks. Then, we analyze the process of canceling each source's own signal from the received network coded signal.

4.4.1   Set a threshold

As the probability distribution of the soft information at the relay is varied according to the source-to-relay channel SNR, we force the relay to evaluate the quality of the received signals by checking whether the received signals satisfy the preset requirement. When the TCQ codewords are repeated, the only codewords 1 and -1 are just the BPSK symbols of the DF protocol. To prevent erroneous decisions in the DF protocol from propagating to the receivers, we set a threshold based on the instantaneous BER of each received block; it is computed as

$$P_{e-i\mathcal{R}} = Q\left(\sqrt{E_i h_{i\mathcal{R}}^2/\sigma^2}\right), \tag{4.9}$$

where $Q\left(\cdot\right)$ is a Q-function [85, (4.1)], and the content inside the Q-function denotes the SNR of the source-to-relay channel.

In this work, we predetermine a BER threshold at the relay, so as to switch between different transmission schemes. If the instantaneous BER is smaller than the predetermined BER threshold, P_{th}, the source-to-relay transmission is deemed to be highly reliable and the soft information centralizes on 1 and -1. In the TWRC, according to Eq. (2.4), the network coded symbols are equivalent to 1 and -1 as long as both received blocks from the two sources are highly reliable. So we use the EF with TCQ codewords repeat scheme when

both $P_{e-1\mathcal{R}}$ and $P_{e-2\mathcal{R}}$ are smaller than P_{th}. Otherwise, the EF with TCQ scheme using codebooks generated from the Lloyd algorithm is utilized. That is,

$$
\text{Relay Strategy} = \begin{cases} \text{EF with TCQ codewords repeat} & \text{if } P_{e-i\mathcal{R}} < P_{th} \\ \text{EF with TCQ} & \text{Otherwise} \end{cases}.
$$

Setting the certain BER as a threshold is equivalent to setting the corresponding source-to-relay channel SNR as a threshold according to Eq. (4.9). In practice, the threshold can be eliminated because codebooks are predetermined at both the relay and receivers based on the different source-to-relay channel SNRs.

4.4.2   Cancel the source's own signal

The received quantized signal at each receiver has been defined in Eq. (4.3), which is then multiplied with x_i so as to cancel x_i. We follow the method for the EF protocol in [77], the estimated symbol of x_i^q is defined as $\hat{x}_i^q = \psi_i \left(x_i^q + e_i \right)$, where e_i denotes the uncorrelated soft noise, and ψ_i represents the scalar factor which makes the soft noise e_i uncorrelated to the information symbol x_i^q, namely, $\mathcal{E}\left(e_i x_i^q \right) = 0$, and $\psi_i = \frac{\mathcal{E}\left(x_i^q * \hat{x}_i^q \right)}{\mathcal{E}\left(x_i^q * x_i^q \right)}$. Besides, we define $\beta = \sqrt{E_R / \mathcal{E}\left(\left| \tanh\left(\frac{LLR_{x_{1,\mathcal{R}}^q}}{2} \right) \tanh\left(\frac{LLR_{x_{2,\mathcal{R}}^q}}{2} \right) \right|^2 \right)}$, hence the canceling process can be expressed as

$$
\begin{aligned}
x_i^q \hat{f}^*(y_{1\mathcal{R}}^q, y_{2\mathcal{R}}^q) &= \beta \hat{x}_1^q \hat{x}_2^q x_i^q + n_{equiv\_\mathcal{R}i}^q x_i^q \\
&= \beta \psi_1 \psi_2 x_j^q + \beta \psi_1 \psi_2 \left(e_j + x_i^q x_j^q e_i + x_i^q e_i e_j \right) + n_{equiv\_\mathcal{R}i}^q x_i^q, \quad (4.10)
\end{aligned}
$$

where we define the noise item, i.e. $N_i \triangleq \beta \psi_1 \psi_2 \left(e_j + x_i^q x_j^q e_i + x_i^q e_i e_j \right) + n_{equiv\_\mathcal{R}i}^q x_i^q$, and we regard it as approximately Gaussian distributed with the mean value m_{N_i} and the variance $\sigma^2_{N_i}$. The employment of the TCQ is a realization of the minimum mean-square error quantizer. Since the mean value of the output of a minimum mean-square error quantizer is equal to the mean value of the input; thus, the mean value of the quantization noise is 0. Besides, since $\mathcal{E}\left(e_i x_i^q \right) = 0$, we have $m_{N_i} = 0$ and $\sigma^2_{N_i} = \beta^2 \psi_1^2 \psi_2^2 \left(\sigma^2_{e_1} + \sigma^2_{e_2} + \sigma^2_{e_1} \sigma^2_{e_2} \right) + \sigma^2_{equiv\_\mathcal{R}i}$, where $\sigma^2_{e_i}$ denotes the variance of the soft noise e_i, and $\sigma^2_{equiv\_\mathcal{R}i}$ represents the variance of the quantization noise, which is a statistic in practical situations.
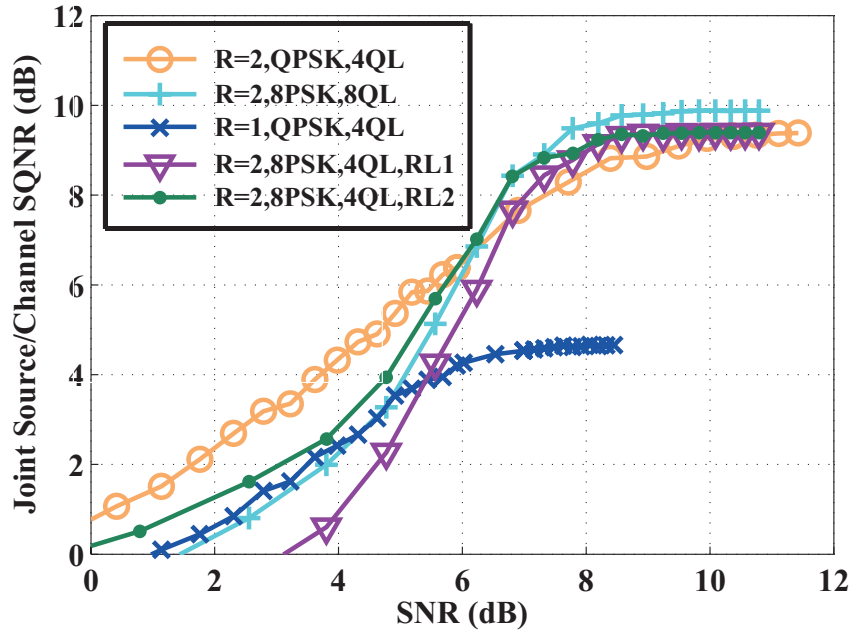
Figure 4.6: Joint TCQ/TCM performance (SQNR) versus SNR for a memoryless Gaussian source and 4-state trellis over AWGN channel (QL: quantization levels, RL1: $(1 = 6, 2 = 7, 3 = 8, 4 = 5)$, RL2: $(1 = 8, 2 = 7, 3 = 6, 4 = 5)$).

4.5 Simulation Results

4.5.1 Memoryless Gaussian Source

The simulation for memoryless Gaussian source consists of 20 times trellis coded quantization of 1000 samples of a zero-mean, unit variance memoryless Gaussian source, followed by the trellis coded modulation of both situations we mentioned above at each SNR established and then calculates the corresponding average signal quantization noise ratio (SQNR), which is expressed in decibels as

$$SQNR = 10\log_{10}\left(\sigma^2{}_X / \rho_n\left(x, \hat{x}\right)\right)$$

Fig. 4.6 summarizes the overall source/channel performance as a function of SNR. As can be seen, firstly for conventional TCQ/TCM, namely the scheme with encoding rate R and corresponding 2^{R+1} quantization levels and 2^{R+1} modulation symbols, the performance at

encoding rate 1 b/sample is slightly better than the performance at encoding rate 2 b/sample under low channel SNR. The reason is that when channel SNR is quite low, with a rate-$1/2$ convolutional encoder for both $R = 1$ and $R = 2$, the overall convolutional encoding rate is $1/2$ and $2/3$, respectively. Besides, rate-$1/2$ is more protective against errors with 2 bits shielding 1 bit, while the other one is with 3 bits shielding 2 bits. Secondly, for TCQ/TCM with repeat rule, simulations counted for this situation are all based on $R = 2$. We first consider the scenario where QPSK is used as the modulation scheme. Under low channel SNR, with quantization level repeating, it still keeps all 2^R quantization levels that $R = 1$ has, which shows that it should perform no worse than $R = 1$, but on the contrary, much better than $R = 1$. This can be seen in Fig. 4.6, and thus the TCQ/TCM with codewords repeat scheme outperforms conventional TCQ/TCM at $R = 2$ under low channel SNR. As the channel SNR increases, all kinds of performance incline towards stableness. Performance of conventional TCM/TCQ at $R = 2$ keeps less than 1 dB better than that of TCM/TCQ with quantization level repeating when they both get stable. The reason is that with fewer errors occurring in the channel, conventional TCM/TCQ at $R = 2$ has 8 quantization outputs while TCM/TCQ with quantization level repeating at $R = 2$ has only actual 4 quantization outputs, the accuracy loss of the latter one is apparently much more than the former one. Thirdly, in terms of the scenario where 8PSK is used as the modulation scheme, different mapping lead to different performance as the figure shows the performance of repeat rules of $(1 = 6, 2 = 7, 3 = 8, 4 = 5)$ and $(1 = 8, 2 = 7, 3 = 6, 4 = 5)$. Different repeat rules result in the changes of Euclidean distance of the modulation symbols, thus leading to different overall performance. While ultimately only 4 quantization outputs exist under these two conditions, when performance gets stable, it becomes consistent with TCQ/M with quantization level repeating using QPSK.

4.5.2   Soft Information Delivery in TWRC

In the simulation, we consider Rayleigh fading channels. During each transmission period, each source transmits one block which contains 1000 binary symbols. Channels between the sources and the relay, namely $h_{1\mathcal{R}}$, $h_{2\mathcal{R}}$, $h_{\mathcal{R}1}$, $h_{\mathcal{R}2}$, are all with unit variance. Channels between the two sources, i.e. h_{12}, h_{21}, are both with the variance of 0.36. Besides, the transmission power and the receiver noise variance at both the relay and the sources are assumed to be equal. In the simulation, we set the threshold P_{th} to be $1/1000$. At the
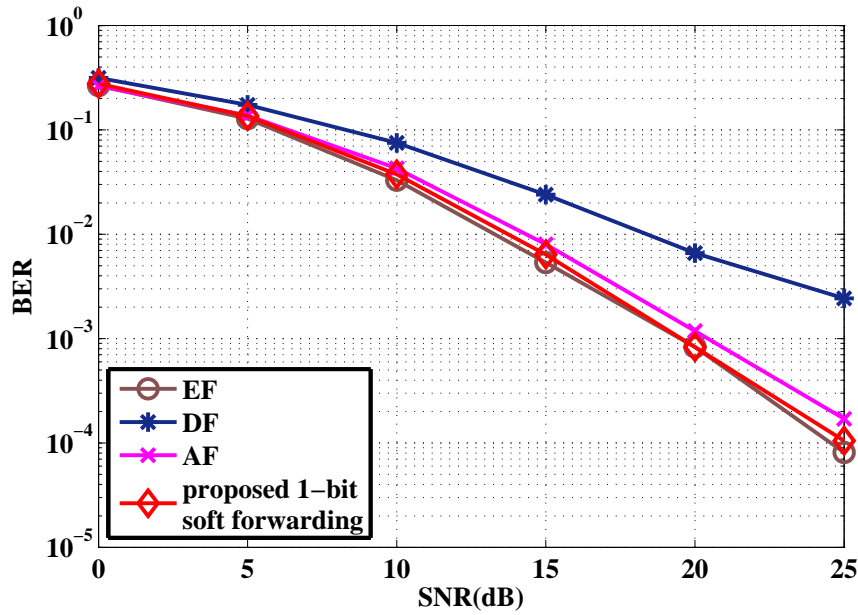
Figure 4.7: BER performance of the proposed soft forwarding scheme over fading channels.

relay, if the instantaneous BER of the received signal is less than the threshold P_{th}, the EF with TCQ codewords repeat scheme is applied. Otherwise, the EF with TCQ scheme using the codebook generated by the Lloyd-Max quantizer is used. The TCQ/M system employs a rate-$1/2$ convolutional encoder shown in the left side of Fig. 2.6. We apply the QPSK constellation with natural mapping in the TCM and choose the codebook of [-1 1 1 -1] for the EF with TCQ codewords repeat scheme, as discussed in Section 4.3. Finally, we take the system BER as the average value of BERs calculated at the two sources.

The AF, DF and EF protocols are taken as benchmarks in the simulation. In Fig. 4.7, X axis denotes the transmission SNR, i.e. E_S/σ^2. As can be seen from Fig. 4.7, both with transmission rate 1, the DF protocol has only one diversity gain, but the proposed protocol can achieve full diversity. Furthermore, the proposed protocol has about 1 dB coding gain compared to the AF protocol at a BER of 10^{-3}. With the increase of the SNR, the probability that the instantaneous BER of the received signals falls below the threshold increases, thus the times of operating the EF with TCQ codewords repeat scheme will grow, and the performance of this protocol approximates more towards that of the EF protocol in the high SNR region.

In addition, when the EF with TCQ codewords repeat scheme is performed, the codewords of
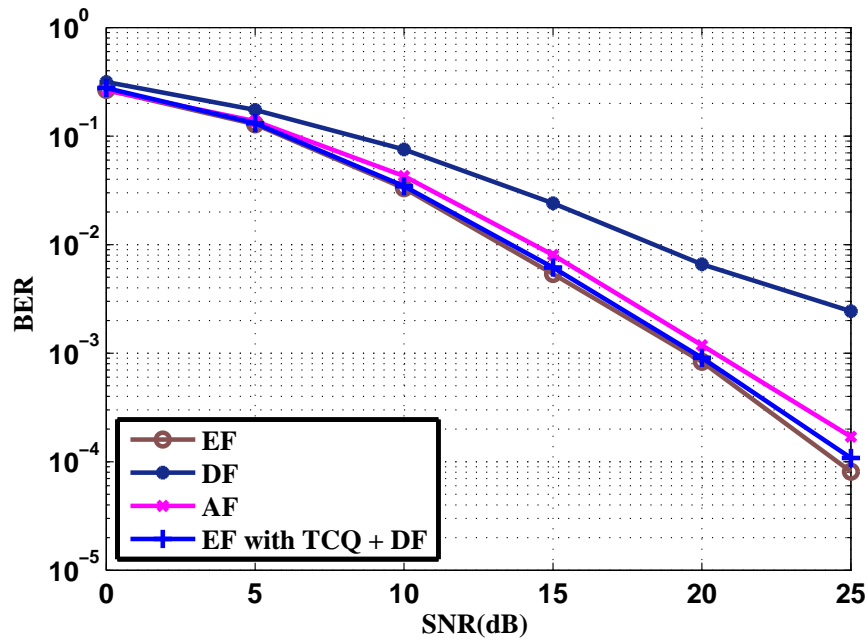
Figure 4.8: BER performance of replaced DF scheme over fading channels.

the value 1 and -1 are exactly the same as the BPSK symbols of the DF protocol transmitted from the relay nodes; therefore, we simulate the scenario where the TCQ codewords repeat scheme is replaced by a simple DF scheme, and the simulation results are shown in Fig. 4.8. The AF, DF and conventional EF protocols are also taken as benchmarks. We can see that EF with TCQ combined with DF scheme achieves full diversity gain, i.e. 2 for TWRC, and outperforms both DF and AF schemes. The two schemes, namely consistently using the EF with TCQ scheme but switching between different codebooks and switching between the EF with TCQ scheme and the DF scheme, have similar BER performance. This owes to the fact that when adopting either codewords repeat scheme or the DF scheme, the instantaneous BER of the received signals at the relay falls below certain threshold, alternatively it means that the channel conditions are very good that wrong decisions would not be made at the relay. Compared with the codewords repeat combined scheme, the DF combined scheme would save time for the relay nodes, as no coding or trellis routing should be experienced, while the frequent switching between different schemes would add more cost to the industrial implementation.

Chapter 5

Conclusions and Future Work

In this thesis, a soft relaying protocol for correlated sources and a practical soft information delivery scheme have been proposed. They are designed for the purpose of enhancing spectral efficiency, network coverage, system reliability, and implementation feasibility of the future wireless networks.

5.1 Conclusions

Chapter 3 has presented an estimated-and-forward technique for correlated sources in an MARC and has exploited the sources' correlation at the relay by implementing CS on the soft bits. We first have developed the expression of the soft bits of the CEF protocol and have proved that the CEF protocol outperforms the conventional EF protocol theoretically. Then we shift the soft bits by subtracting one from all the soft bit values in order to obtain sparsity, and take advantage of a sparse $m \times l$ matrix to generate the linear combinations of the shifted soft bits. Belief propagation is utilized to perform decoding, which requires the prior knowledge of the PDF of the soft bits for different SNRs at the destination. In the simulations, we have compared the proposed CEF protocol with the conventional EF protocol and have made comparison between the CEF-CS protocol at different rates over fading channels, as well as with different correlation models. In addition, the CEF-CS protocol is compared with the uncompressed protocols in terms of the receiver SNR, BER and throughput performance.

Simulation results show that, firstly, the CEF protocol outperforms the EF protocol at all times. Secondly, with the decrease of the source correlation, the network coded symbol vector at the relay node becomes less sparse; consequently the recovery of a less sparse vector is less reliable, and the CEF-CS protocol leads to a worse BER performance; when the correlation related parameter τ falls below 0.3, the proposed protocol can promise a diversity gain of two, while when τ exceeds the value of 0.5, only a diversity gain of one can be achieved. Thirdly, with the increase of the transmission rate of CS at the relay, more information is relayed to the destination node, thus the recovery of the network coded symbols is more reliable, and the CEF-CS protocol leads to a better BER performance; while with the transmission rate increasing, the improvement space becomes smaller due to the suboptimal combining of the signals at the destination; when the transmission rate exceeds 0.5, the CEF-CS protocol obtains a diversity gain of two, while when the transmission rate drops below 0.3, only a diversity gain of one is obtained. Fourthly, in terms of the receiver SNR, the performance of the CEF-CS protocol varies according to different transmission rates; with a higher transmission rate at the relay, the receiver SNR becomes higher; to a certain extent, the receiver SNR of the CEF-CS protocol can exceed the conventional EF protocol. Additionally, the conventional EF protocol is proved to be not suitable for compressive sensing; when CS is applied to the EF protocol, the system only achieves a diversity gain of one regardless of the transmission rates, and the BER performance stays poorer than the CEF-CS protocol all the time. Last but not least, because of the compression adopted at the relay node for the CEF-CS protocol, the transmission time is reduced according to different compression rates; as a result, when the CEF-CS protocol can achieve equivalent error performance to the conventional EF protocol, the CEF-CS protocol can achieve a higher throughput due to less transmission time; at a transmission rate of 0.7, the throughput performance of the CEF-CS protocol is shown to outperform that of the EF protocol by 10%.

In Chapter 4, we have proposed a practical 1-bit soft forwarding protocol in the TWRC. We have taken advantage of the joint TCQ/M scheme to forward the soft information. We have derived the PDF expression of the network coded soft symbol at the relay node; when the source-to-relay channel SNR is low, we apply the Lloyd algorithm to generating the codebook for the TCQ. When the source-to-relay channel SNR is high enough that the soft information is equivalent to its hard decision, we propose to use the EF with TCQ codewords repeat scheme to implement the information delivery at the relay. We have analyzed the application of the codewords repeat scheme by explaining both rate 1 and rate 2 sce-

narios. We have found that the proposed protocol outperforms the AF protocol and the DF protocol over the Rayleigh fading TWRC; both with transmission rate 1, the DF protocol has only one diversity gain, but the proposed protocol can achieve full diversity; it also has about 1 dB coding gain compared to the AF protocol at a BER of 10^{-3}. Besides, it well approximates the EF protocol which assumes the soft information can be forwarded to the receivers without quantization. Additionally, when the soft information is equivalent to the hard decisions of the received signal under high source-to-relay channel SNRs, the DF protocol can also be utilized. Simulation results show that combining the two schemes, namely EF with TCQ and DF, can also achieve a diversity gain of two over fading channels. The disadvantage of this scheme is that switching between two different schemes increases the cost of implementation.

The proposed protocols can be generalized to any relay networks with more than one source node. However, in terms of their feasibility in practice, different protocols are designed to aim at different practical scenarios. The CEF-CS protocol achieves much better performance when the sources are highly correlated. This is not a common case in TWRC, while in MARC adjacent source nodes observe a single event and collect correlated information. In Chapter 4, for the 1-bit soft forwarding protocol, my aim is to investigate a practical delivery method of soft information in cellular networks as it is not yet discussed in the existing literature, and TWRC is a common model for cellular networks. Theoretically, the 1-bit soft forwarding protocol can be directly applied to the MARC.

5.2   Future Work

First of all, all of works within this thesis are based on uncoded systems. As is known, to separate coded system from the uncoded system is to judge whether channel coding techniques are incorporated in the data transmission or not. Authors in [76, 86, 87] already considered the coded relay systems, and it is demonstrated that system performance depends not only on the forwarding protocol, but also on the distributed coding design. However, throughout this thesis, the signals transmitted from the source nodes are assumed to be without any channel code. For the CEF-CS protocol proposed in Chapter 3, if channel code can be added to the transmitted symbols at the source nodes, a joint decoder at the destination node can be designed to further improve the system performance; LDPC can be a good option, as the

CS operation at the relay node utilizes an LDPC like matrix and BP is used at the destination node, then the BP decoder can be designed to jointly decode the coded signals from the source nodes and the compressed signals from the relay node. For the 1-bit soft forwarding protocol proposed in Chapter 4, we can add an interleaver and a convolution encoder after the TCQ encoder at the relay. We consider to use turbo TCM to modulate the symbols output from the convolutional encoder. At the destination, we can use iterative decoding algorithms to decode the source information, thus, enhance the overall system performance.

Secondly, Chapter 3 still proposes a soft information forwarding technique, which again causes the problem of actual delivery of the soft information. Even if we combine the soft information delivery scheme proposed in Chapter 4 together, the overall system will be not efficient, resulting in much delay caused by a large number of computing. However, in the literature, 1-bit Compressive Sensing techniques have already been drawn much attention [88–90] and point out our future research focus. We can design a 1-bit CS related relay protocol to both achieve good performance and save channel bandwidth.

Appendix A

Proofs for Chapter 3

A.1 Proof of *Theorem 1*

We further develop the soft symbol $\tilde{x}_{\mathcal{R}}^j$ in (3.4) as

$$\tilde{x}_{\mathcal{R}}^j = \frac{\alpha\left(2 - \tau\right) - \theta\tau}{\alpha\left(2 - \tau\right) + \theta\tau},\tag{A.1}$$

where

$$\alpha = \sum_{x_1^j x_2^j = 1} p\left(y_{1\mathcal{R}}^j | x_1^j\right) p\left(y_{2\mathcal{R}}^j | x_2^j\right), \text{ and } \quad \theta = \sum_{x_1^j x_2^j = -1} p\left(y_{1\mathcal{R}}^j | x_1^j\right) p\left(y_{2\mathcal{R}}^j | x_2^j\right).\tag{A.2}$$

Obviously, we have $\alpha > 0$ and $\theta > 0$.

The conventional EF derives $\tilde{x}_{\mathcal{R}}^j$ in (3.9) by assuming that the two sources are independent, i.e., (3.9) can be obtained by considering $\tau = 1$ in (A.1). In the CEF-CS protocol, we derive $\tilde{x}_{\mathcal{R}}^j$ by considering the real τ. In correlated sources, we always have $\tau < 1$. Given α and θ, $\tilde{x}_{\mathcal{R}}^j$ can be regarded as a function of τ, which is denoted by $\delta\left(\tau\right)$. To investigate the relationship between $\delta\left(\tau\right)$ and τ, we derive the first-order derivative of $\delta\left(p\right)$ as follows.

$$\frac{\mathrm{d}\delta\left(\tau\right)}{\mathrm{d}\tau} = \frac{-8\alpha\theta}{\left(\alpha(2 - \tau) + \theta\tau\right)^2}.\tag{A.3}$$

A.1 Proof of *Theorem 1*

Since $\alpha > 0$ and $\theta > 0$, we always have $\frac{\mathrm{d}\delta(\tau)}{\mathrm{d}p} < 0$, which meas that $\delta(\tau)$ is a decreasing function in terms of τ. When correlation exists between the sources, we have $\tau < 1$. Therefore, the soft symbol values in the CEF protocol are always larger than that in the conventional EF protocol. As the majority of the soft symbols $\tilde{x}_{\mathcal{R}}^{j}$ approach the value of 1, the soft symbols in the CEF protocol are more reliable than those of the EF protocol.

Bibliography

[1] J. G. Proakis and M. Salehi, *Digital Communications*, 5th ed. McGraw-Hill, 2008.

[2] E. Telatar, "Capacity of multi-antenna Gaussian channels," *Europ. Trans. Telecomm.*, vol. 10, pp. 585–595, Nov/Dec 1999.

[3] V. Tarokh, N. Seshadri, and A. Calderbank, "Space-time codes for high data rate wireless communication: performance criterion and code construction," *IEEE Trans. Inf. Theory*, vol. 44, no. 2, pp. 744–765, 1998.

[4] E. Biglieri, J. Proakis, and S. Shamai, "Fading channels: information-theoretic and communications aspects," *IEEE Trans. Inf. Theory*, vol. 44, no. 6, pp. 2619–2692, 1998.

[5] Y. Li, "Distributed coding for cooperative wireless networks: An overview and recent advances," *IEEE Commun. Mag.*, vol. 47, no. 8, pp. 71–77, 2009.

[6] A. Sendonaris, E. Erkip, and B. Aazhang, "User cooperation diversity. Part I. System description," *IEEE Trans. Commun.*, vol. 51, no. 11, pp. 1927–1938, Nov. 2003.

[7] E. C. V. D. Meulen, "Three-terminal communication channels," *Advances in Applied Probability*, vol. 3, no. 1, pp. 120–154, 1971.

[8] T. M. Cover and A. A. E. Gamal, "Capacity theorems for the relay channel," *IEEE Trans. Inform. Theory*, vol. IT-25, pp. 572–584, Sep. 1979.

[9] H. Wu, C. Qiao, S. De, and O. Tonguz, "Integrated cellular and ad hoc relaying systems: iCAR," *IEEE J. Sel. Areas Commun.*, vol. 19, no. 10, pp. 2105–2115, 2001.

[10] K. Zheng, B. Fan, Z. Ma, G. Liu, X. Shen, and W. Wang, "Multihop cellular networks toward LTE-advanced," *IEEE Veh. Technol. Mag.*, vol. 4, no. 3, pp. 40–47, Sep. 2009.

[11] H. Viswanathan and S. Mukherjee, "Performance of cellular networks with relays and centralized scheduling," *IEEE Trans. Wireless Commun.*, vol. 4, no. 5, pp. 2318–2328, 2005.

[12] I. Bouazizi, K. Jarvinen, and M. Hannuksela, "3gpp mobile multimedia services [standards in a nutshell]," *Signal Processing Magazine, IEEE*, vol. 27, no. 5, pp. 125–130, 2010.

[13] I. F. Akyildiz, S. Weilian, Y. Sankarasubramaniam, and E. Cayirci, "A survey on sensor networks," *IEEE Commun. Mag.*, vol. 40, no. 8, pp. 102–114, 2002.

[14] E. L. Lloyd and X. Guoliang, "Relay node placement in wireless sensor networks," *IEEE Trans. Comput.*, vol. 56, no. 1, pp. 134–138, 2007.

[15] S. Misra, S. D. Hong, G. Xue, and J. Tang, "Constrained relay node placement in wireless sensor networks to meet connectivity and survivability requirements," in *The 27th IEEE Conference on Computer Communications (INFOCOM)*, 2008.

[16] R. Ahlswede, N. Cai, S. Y. R. Li, and R. W. Yeung, "Network information flow," *IEEE Trans. Inform. Theory*, vol. 46, no. 4, pp. 1204 –1216, July 2000.

[17] S. Y. R. Li, R. W. Yeung, and N. Cai, "Linear network coding," *IEEE Trans. Inform. Theory*, vol. 49, no. 2, Feb. 2003.

[18] R. W. Yeung, S. Y. R. Li, N. Cai, and Z. Zhang, *Network Coding Theory*. Now Publishers Inc., 2006.

[19] Y. Wu, P. A. Chou, and S. Y. Kung, "Information exchange in wireless networks with network coding and physical-layer broadcast," in *Technical Report MSR-TR-2004-78, Microsoft Research*, Redmond, WA, Aug. 2004.

[20] S. Zhang and S. C. Liew, "Channel coding and decoding in a relay system operated with physical-layer network coding," *IEEE J. Sel. Areas Commun.*, vol. 27, no. 5, pp. 788–796, Jun. 2009.

[21] S. Zhang, S. C. Liew, and P. Lam, "Physical layer network coding," in *Proc. ACM MOBICOM*, Los Angeles, 2006.

[22] B. Nazer and M. Gastpar, "Reliable physical layer network coding," *Proc. IEEE*, vol. 99, no. 3, pp. 438–460, 2011.

[23] R. H. Y. Louie, Y. Li, and B. Vucetic, "Practical physical layer network coding for two-way relay channels: performance analysis and comparison," *IEEE Trans. Wireless Commun.*, vol. 9, no. 2, pp. 764 –777, Feb. 2010.

[24] J. N. Laneman, D. N. C. Tse, and G. W. Wornell, "Cooperative diversity in wireless networks: Efficient protocols and outage behavior," *IEEE Trans. Inf. Theory*, vol. 50, no. 12, pp. 3062–3080, Dec. 2004.

[25] C. Deqiang and J. N. Laneman, "Modulation and demodulation for cooperative diversity in wireless systems," *IEEE Trans. Wireless Commun.*, vol. 5, no. 7, pp. 1785–1794, 2006.

[26] Y. Li, B. Vucetic, T. Wong, and M. Dohler, "Distributed turbo coding with soft information relaying in multihop relay networks," *IEEE J. Sel. Areas Commun.*, vol. 24, no. 11, pp. 2040–2050, Nov. 2006.

[27] K. S. Gomadam and S. A. Jafar, "Optimal relay functionality for snr maximization in memoryless relay networks," *IEEE J. Sel. Areas Commun.*, vol. 25, no. 2, pp. 390–401, Feb. 2007.

[28] J. Li, M. Karim, J. Yuan, Z. Chen, Z. Lin, and B. Vucetic, "Novel soft information forwarding protocols in two-way relay channels," *IEEE Trans. Veh. Technol.*, vol. 62, no. 5, pp. 2374–2381, Jun. 2013.

[29] M. A. Karim, J. Yuan, Z. Chen, and J. Li, "Soft information relaying in fading channels," *IEEE Wireless Commun. Lett.*, vol. 1, no. 3, pp. 233–236, Jun. 2012.

[30] J. Li, J. Yuan, R. Malancy, M. Xiao, and W. Chen, "Full-diversity binary frame-wise network coding for multiple-source multiple-relay networks over slow-fading channels," *IEEE Trans. Veh. Technol.*, vol. 61, no. 3, pp. 1346–1360, Mar. 2012.

[31] M. Xiao, J. Kliewer, and M. Skoglund, "Design of network codes for multiple-user multiple-relay wireless networks," *IEEE Trans. Commun.*, vol. 60, no. 12, pp. 3755–3766, Dec. 2012.

[32] J. Barros and S. D. Servetto, "Network information flow with correlated sources," *IEEE Trans. Inf. Theory*, vol. 52, no. 1, pp. 155–170, 2006.

[33] L. Ong, R. Timo, and S. Johnson, "The finite field multi-way relay channel with correlated sources: Beyond three users," in *2012 IEEE International Symposium on Information Theory Proceedings (ISIT)*, 2012, pp. 791–795.

[34] M. Karim, T. Yang, J. Yuan, Z. Chen, and I. Land, "A novel soft forwarding technique for memoryless relay channels based on symbol-wise mutual information," *IEEE Commun. Lett.*, vol. 14, no. 10, pp. 927–929, 2010.

[35] M. Karim, J. Yuan, Z. Chen, and J. Li, "Analysis of mutual information based soft forwarding relays in awgn channels," in *IEEE Global Telecommunications Conference (GLOBECOM 2011)*, 2011, pp. 1–5.

[36] C. Hausl and J. Hagenauer, "Iterative network and channel decoding for the two-way relay channel," in *2006 IEEE International Conference on Communications (ICC)*, vol. 4, 2006, pp. 1568–1573.

[37] G. Wang, W. Xiang, and J. Yuan, "Multihop compute-and-forward for generalized two-way relay channels," *Transactions on emerging telecommunications technologies*, pp. 1–13, In Press.

[38] S. Zhang, Y. Zhu, and S. C. Liew, "Soft network coding in wireless two-way relay channels," *J. Communication and Networks, Special Issues on Network Coding*, vol. 10, no. 4, 2008.

[39] C. Tao, T. Ho, and J. Kliewer, "Memoryless relay strategies for two-way relay channels," *IEEE Trans. Commun.*, vol. 57, no. 10, pp. 3132–3143, 2009.

[40] C. Shannon, "Two-way communication channels," in *Proc. 4th Berkeley Symp. Math. Sta. Prob.*, vol. 1, 1961, pp. 611–644.

[41] B. Rankov and A. Wittneben, "Spectral efficient protocols for half-duplex fading relay channels," *IEEE J. Select. Areas Commun.*, vol. 25, no. 2, pp. 379 –389, Feb. 2007.

[42] J. N. Laneman, D. N. C. Tse, and G. W. Wornell, "Cooperative diversity in wireless networks: efficient protocols and outage behavior," *IEEE Trans. Inform. Theory*, vol. 50, no. 12, pp. 3062–3080, Dec. 2004.

[43] N. Yang, P. L. Yeoh, M. Elkashlan, I. B. Collings, and Z. Chen, "Two-way relaying with multi-antenna sources: beamforming and antenna selection," *IEEE Trans. Veh. Technol.*, vol. 61, no. 9, pp. 3996 –4008, Nov. 2012.

[44] A. Sprintson, "Network coding and its applications in communication networks," *Algorithms for Next Generation Networks*, pp. 343–372, 2010.

[45] S. Katti, H. Rahul, W. Hu, D. Katabi, M. Medard, and J. Crowcroft, "Xors in the air: practical wireless network coding," *IEEE/ACM Transactions on Networking*, vol. 16, no. 3, pp. 497 –510, June 2008.

[46] Y. Han, S. H. Ting, C. K. Ho, and W. H. Chin, "High rate two-way amplify-and-forward half-duplex relaying with OSTBC," in *Proc. IEEE VTC*, Singapore, May 2008, pp. 2426–2430.

[47] C. Hausl and P. Dupraz, "Joint network-channel coding for the multiple-access relay channel," in *3rd Annual IEEE Communications Society on Sensor and Ad Hoc Communications and Networks (SECON)*, 2006, pp. 817–822.

[48] D. Woldegebreal and H. Karl, "Multiple-access relay channel with network coding and non-ideal source-relay channels," in *4th International Symposium on Wireless Communication Systems*, 2007, pp. 732–736.

[49] G. Kramer and A. Van Wijngaarden, "On the white gaussian multiple-access relay channel," in *IEEE International Symposium on Information Theory*, 2000, pp. 40–40.

[50] G. Kramer, M. Gastpar, and P. Gupta, "Cooperative strategies and capacity theorems for relay networks," *IEEE Trans. Inf. Theory*, vol. 51, no. 9, pp. 3037–3063, Sep. 2005.

[51] R. DeVore, B. Jawerth, and B. Lucier, "Image compression through wavelet transform coding," *IEEE Trans. Inf. Theory*, vol. 38, no. 2, pp. 719–746, 1992.

[52] I. Gorodnitsky and B. Rao, "Sparse signal reconstruction from limited data using FOCUSS: a re-weighted minimum norm algorithm," *IEEE Trans. Signal Process.*, vol. 45, no. 3, pp. 600–616, 1997.

[53] E. J. Candes, J. Romberg, and T. Tao, "Robust uncertainty principles: exact signal reconstruction from highly incomplete frequency information," *IEEE Trans. Inf. Theory*, vol. 52, no. 2, pp. 489–509, 2006.

[54] D. L. Donoho, "Compressed sensing," *IEEE Trans. Inf. Theory*, vol. 52, no. 4, pp. 1289–1306, 2006.

[55] E. J. Candes and M. B. Wakin, "An introduction to compressive sampling," *IEEE Signal Process. Mag.*, vol. 25, no. 2, pp. 21–30, 2008.

[56] M. A. S. Scott Shaobing Chen, David L. Donoho, "Atomic decomposition by basis pursuit," *SIAM Journal on Scientific Computing*, vol. 20, no. 1, pp. 33–61, 1998.

[57] J. Tropp and A. Gilbert, "Signal recovery from random measurements via orthogonal matching pursuit," *IEEE Trans. Inf. Theory*, vol. 53, no. 12, pp. 4655–4666, 2007.

[58] D. Baron, S. Sarvotham, and R. G. Baraniuk, "Bayesian compressive sensing via belief propagation," *IEEE Trans. Signal Process.*, vol. 58, no. 1, pp. 269–280, 2010.

[59] E. Candes, M. Rudelson, T. Tao, and R. Vershynin, "Error correction via linear programming," in *46th Annual IEEE Symposium on Foundations of Computer Science, 2005*, 2005, pp. 668–681.

[60] D. Guo and C.-C. Wang, "Multiuser detection of sparsely spread CDMA," *IEEE J. Sel. Areas Commun.*, vol. 26, no. 3, pp. 421–431, 2008.

[61] S. Sarvotham, D. Baron, and R. G. Baraniuk, "Sudocodes - fast measurement and reconstruction of sparse signals," in *IEEE International Symposium on Information Theory (ISIT)*, 2006, pp. 2804–2808.

[62] S.-Y. Chung, T. J. Richardson, and R. L. Urbanke, "Analysis of sum-product decoding of low-density parity-check codes using a Gaussian approximation," *IEEE Trans. Inf. Theory*, vol. 47, no. 2, pp. 657–670, Feb. 2001.

[63] T. J. Richardson and R. L. Urbanke, "The capacity of low-density parity-check codes under message-passing decoding," *IEEE Trans. Inf. Theory*, vol. 47, no. 2, pp. 599–618, Feb. 2001.

[64] D. J. MacKay, *Information theory, inference and learning algorithms*. Cambridge university press, 2003.

[65] M. Pretti, "A message-passing algorithm with damping," *Journal of Statistical Mechanics*, 2005.

[66] G. Ungerboeck, "Channel coding with multilevel/phase signals," *IEEE Trans. Inf. Theory*, vol. 28, no. 1, pp. 55–67, 1982.

[67] ——, "Trellis-coded modulation with redundant signal sets part i: Introduction," *IEEE Commun. Mag.*, vol. 25, no. 2, pp. 5–11, 1987.

[68] M. W. Marcellin and T. R. Fischer, "Trellis coded quantization of memoryless and gauss-markov sources," *IEEE Trans. Commun.*, vol. 38, no. 1, pp. 82–93, 1990.

[69] A. J. Viterbi, "Error bounds for convolutional codes and an asymptotically optimum decoding algorithm," *IEEE Trans. Inf. Theory*, vol. 13, pp. 260–269, Apr. 1967.

[70] T. S. Rappaport, *Wireless communications: principles and practice*. Prentice Hall PTR, Feb. 2009.

[71] S. Lloyd, "Least squares quantization in PCM," *IEEE Trans. Inf. Theory*, vol. 28, no. 2, pp. 129–137, 1982.

[72] J. Max, "Quantizing for minimum distortion," *IEEE Trans. Inf. Theory*, vol. 6, pp. 7–12, 1960.

[73] T. R. Fischer and M. W. Marcellin, "Joint trellis coded quantization/modulation," *IEEE Trans. Commun.*, vol. 39, no. 2, pp. 172–176, 1991.

[74] Z. Lin and T. Aulin, "Joint source-channel coding using combined TCQ/CPM: iterative decoding," *IEEE Trans. Commun.*, vol. 53, no. 12, pp. 1991–1995, 2005.

[75] J. N. Laneman, D. N. C. Tse, and G. W. Wornell, "Cooperative diversity in wireless networks: Efficient protocols and outage behavior," *IEEE Trans. Inf. Theory*, vol. 50, no. 12, pp. 3062–3080, 2004.

[76] Y. Li, B. Vucetic, T. F. Wong, and M. Dohler, "Distributed turbo coding with soft information relaying in multihop relay networks," *IEEE J. Sel. Areas Commun.*, vol. 24, no. 11, pp. 2040–2050, 2006.

[77] G. Krishna Srikanth and J. Syed Ali, "Optimal relay functionality for SNR maximization in memoryless relay networks," *IEEE J. Sel. Areas Commun.*, vol. 25, no. 2, pp. 390–401, 2007.

[78] Y. Sichao and R. Koetter, "Network coding over a noisy relay : a belief propagation approach," in *IEEE International Symposium on Information Theory (ISIT)*, 2007, pp. 801–804.

[79] N. Nguyen, D. L. Jones, and S. Krishnamurthy, "Netcompress: Coupling network coding and compressed sensing for efficient data communication in wireless sensor networks," in *Signal Processing Systems (SIPS), 2010 IEEE Workshop on*, 2010, pp. 356–361.

[80] F. Bassi, L. Chao, L. Iwaza, and M. Kieffer, "Compressive linear network coding for efficient data collection in wireless sensor networks," in *20th European Signal Processing Conference (EUSIPCO)*, 2012, pp. 714–718.

[81] A. Yedla, H. D. Pfister, and K. R. Narayanan, "Can iterative decoding for erasure correlated sources be universal?" in *47th IEEE Annual Allerton Conference on Communication, Control, and Computing*, 2009, pp. 408–415.

[82] I. Abou-Faycal and M. Medard, "Optimal uncoded regeneration for binary antipodal signaling," in *2004 IEEE International Conference on Communications (ICC),*, vol. 2, 2004, pp. 742–746 Vol.2.

[83] Z. Lin and T. Aulin, "On joint source and channel coding using trellis coded cpm: Analytical bounds on the channel distortion," *IEEE Trans. Inf. Theory*, vol. 53, no. 9, pp. 3081–3094, 2007.

[84] C. Novak, P. Fertl, and G. Matz, "Quantization for soft-output demodulators in bit-interleaved coded modulation systems," in *2009 IEEE International Symposium on Information Theory (ISIT)*, 2009, pp. 1070–1074.

[85] M. Dan, "Digital communication over fading channels, second edition," p. 160, 2005.

[86] J. N. Laneman and G. W. Wornell, "Distributed space-time-coded protocols for exploiting cooperative diversity in wireless networks," *IEEE Trans. Inform. Theory*, vol. 49, no. 10, pp. 2415–2425, Oct. 2003.

[87] P. Salvo Rossi, A. Petropulu, F. Palmieri, and G. Iannello, "Distributed linear block coding for cooperative wireless communications," *IEEE Signal Process. Lett.*, vol. 14, no. 10, pp. 673–676, 2007.

[88] P. T. Boufounos and R. G. Baraniuk, "1-bit compressive sensing," in *CISS 2008. 42nd Annual Conference on Information Sciences and Systems*, 2008, pp. 16–21.

[89] J. N. Laska, W. Zaiwen, Y. Wotao, and R. G. Baraniuk, "Trust, but verify: Fast and accurate signal recovery from 1-bit compressive measurements," *IEEE Trans. Signal Process.*, vol. 59, no. 11, pp. 5289–5301, 2011.

[90] Y. Ming, Y. Yi, and S. Osher, "Robust 1-bit compressive sensing using adaptive outlier pursuit," *IEEE Trans. Signal Process.*, vol. 60, no. 7, pp. 3868–3875, 2012.